

RSC Advances



This is an *Accepted Manuscript*, which has been through the Royal Society of Chemistry peer review process and has been accepted for publication.

Accepted Manuscripts are published online shortly after acceptance, before technical editing, formatting and proof reading. Using this free service, authors can make their results available to the community, in citable form, before we publish the edited article. This *Accepted Manuscript* will be replaced by the edited, formatted and paginated article as soon as this is available.

You can find more information about *Accepted Manuscripts* in the [Information for Authors](#).

Please note that technical editing may introduce minor changes to the text and/or graphics, which may alter content. The journal's standard [Terms & Conditions](#) and the [Ethical guidelines](#) still apply. In no event shall the Royal Society of Chemistry be held responsible for any errors or omissions in this *Accepted Manuscript* or any consequences arising from the use of any information it contains.

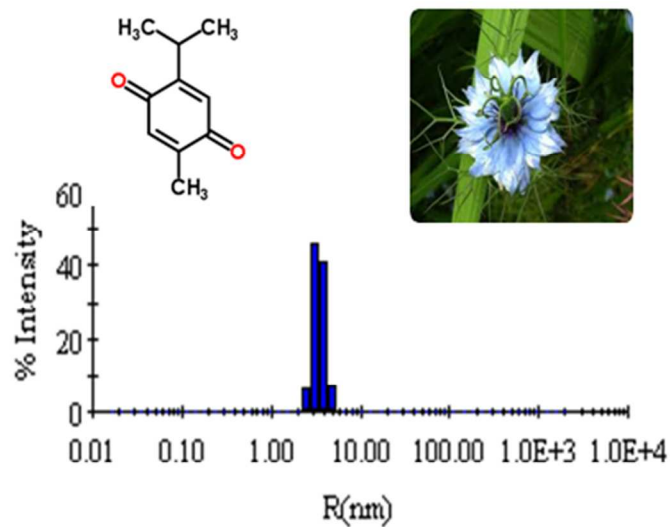
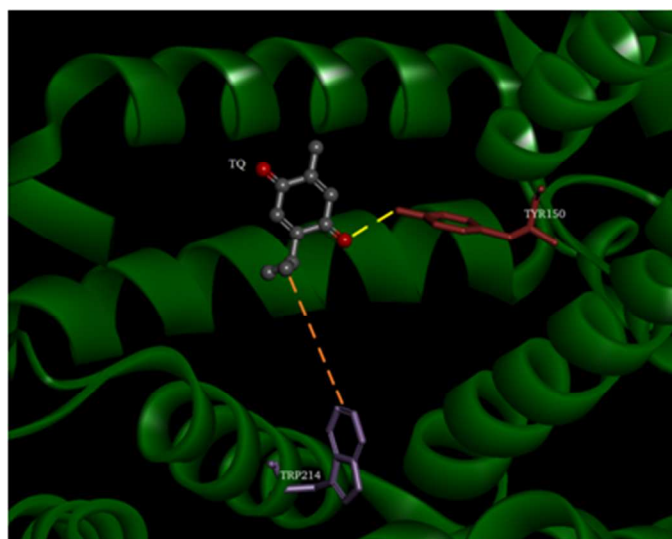
Table of Contents

Biophysical insight of Thymoquinone Binding to 'N' and 'B'-isoforms to explore the Interaction Mechanism and Radical Scavenging Activity

Mohd Ishtikhar¹, Gulam Rabbani¹, Shawez Khan² and Rizwan Hasan Khan^{1*}

¹Interdisciplinary Biotechnology Unit, Aligarh Muslim University, Aligarh – 202002, India

²Department of Computer Science, Jamia Millia Islamia, Jamia Nagar, New Delhi-110025, India



1
2
3
4
5
6
7
8
9
10
11
12
13
14
15
16
17
18
19
20
21
22
23
24
25
26
27
28
29
30
31
32
33

Research Article

Biophysical investigation of thymoquinone binding to ‘N’ and ‘B’ isoform of human serum albumin and explore the interaction mechanism and radical scavenging activity

Mohd Ishtikhar¹, Gulam Rabbani¹, Shawez Khan² and Rizwan Hasan Khan^{1*}

¹Interdisciplinary Biotechnology Unit, Aligarh Muslim University, Aligarh – 202002, India

²Department of Computer Science, Jamia Millia Islamia, Jamia Nagar, New Delhi-110025, India

*To whom correspondence should be addressed

Prof. Rizwan Hasan Khan

Interdisciplinary Biotechnology Unit,

Aligarh Muslim University,

Aligarh-202002

E-mail: rizwanhkhan@hotmail.com

rizwanhkhan1@gmail.com

Phone: +91-571-2727388

Fax: +91-571-2721776

1

2

3

4

5

6

7

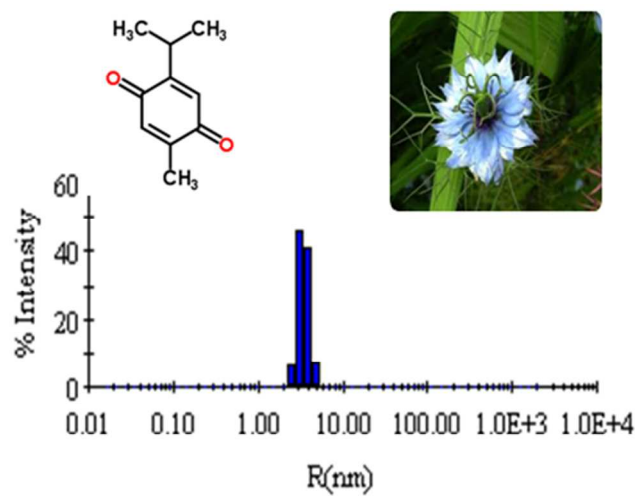
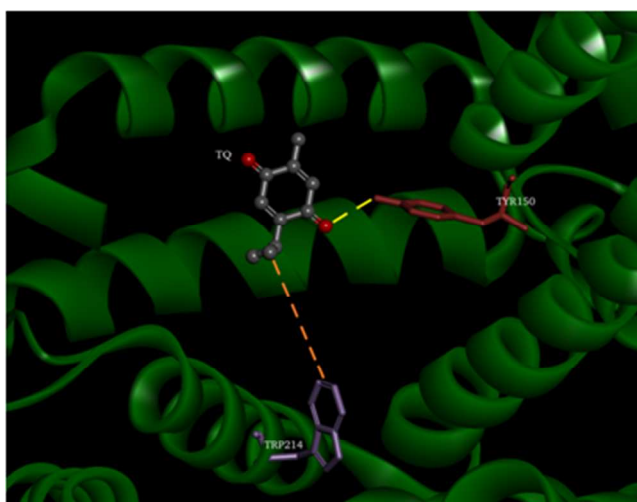
8

9

10

11

TABLE OF CONTENT



12

13

14

15

16 Thymoquinone more strongly interact with the 'N' isoform in comparison to 'B' isoform of HSA

17 and also increase its thermal stability but the antioxidant activity is significantly higher at the 'B'

18

isoform of HSA.

19

20

21

1 **Abstract**

2 Thymoquinone (TQ) is the main constituent of *Nigella sativa* and is traditionally used
3 as folk medicine. Our aim was to investigate the binding mechanism of TQ to human
4 serum albumin (HSA) isoforms ('N' form at pH 7.4 and 'B' form at pH 9.0) using
5 biophysical methods such as intrinsic tryptophan fluorescence quenching, isothermal
6 titration calorimetry (ITC), circular dichroism (CD), dynamic light scattering (DLS),
7 Förster resonance energy transfer (FRET) and antioxidant activity in the absence and
8 presence of TQ. We have calculated the binding and thermodynamic parameters from
9 spectroscopic and calorimetric methods. CD and DLS were respectively used to
10 monitor the changes in the secondary structure and hydrodynamic radii of HSA as a
11 result of its interaction with TQ. The esterase and antioxidant or radical scavenging
12 activities of both the isoforms of HSA were investigated in the absence/presence of TQ.
13 The antioxidant activity of TQ was remarkably enhanced upon its interaction with
14 HSA.. Therefore, the efficiency of HSA to scavenge the free radical ions was increase
15 in the presence of TQ which are generated in the body by various metabolic processes.

16
17
18
19
20 **Abbreviations:** HSA: Human serum albumin; TQ: Thymoquinone; ABTS: 2,2'-Azino-
21 bis (3-ethyl benzothiazoline-6-sulfonic acid) diammonium salt; DLS: Dynamic light
22 scattering; FRET: Förster resonance energy transfer; BHA: Butylated hydroxyanisole;
23 MRE: Mean residual ellipticity.

1 **Keywords:** Antioxidant activity; Esterase activity; Fluorescence spectroscopy; Human
2 serum albumin; Radical scavenging activity; Thymoquinone; Isothermal titration
3 calorimetry.

4

5 **Introduction**

6 Thymoquinone (TQ), a main constituent of *Nigella sativa* (*Ranunculaceae*) essential
7 oil, has been traditionally employed in folk medicine and is now recognized as a herbal
8 remedy by a number of pharmacopoeias ¹. It is an annual plant that grows in the
9 mediterranean area of India and Pakistan. The biochemical activities of *N. sativa* has
10 been ascribed to quinones specifically TQ or 2-isopropyl-5-methyl-1, 4-benzoquinone
11 ². TQ shows antimicrobial ³, anti-inflammatory ⁴, neuroprotective ⁵, antidiabetic,
12 anticancerous ⁶, antihypertensive, and mast cell stabilizing effects ⁷, in addition to a
13 protective role against *in vitro* induced ischemia ^{8,9}. Moreover, the therapeutic potential
14 of TQ has been confirmed in cancer research also ¹⁰⁻¹⁵. TQ has a promising role as
15 antineoplastic growth inhibitor against various tumor cell lines ^{16, 17}. It has protective
16 effects against rheumatoid arthritis ¹⁸, induces telomere shortening, DNA damage,
17 apoptosis in human glioblastoma cells ¹⁹ and triple-negative breast cancer (TNBC)
18 cells ²⁰. TQ also shows anti-oxidative properties against oxidative damage induced by a
19 variety of free radical generating agents (including carbon tetrachloride, *cis*-platin,
20 doxorubicin and recently HIV-1 protease inhibitor) ^{2, 21}, analgesic and anti-
21 inflammatory role against renal injury ²². Because of its immense biological
22 importance, there is an escalating interest to test it in pre-clinical and clinical researches
23 for assessing its health benefits.

1 Human serum albumin (HSA) is a highly abundant serum protein that comprises 50-
2 60% of the total plasma protein in humans²³. Albumin is responsible for the transport,
3 storage and metabolism of many therapeutic drugs in the blood stream thereby
4 restricting their free, active concentrations and therefore can significantly affect their
5 pharmacokinetics²⁴. There are four pH dependent isoforms of HSA that have been
6 characterized in the past. At physiological pH 7.4, HSA assumes the normal form (N)
7 which changes to fast migrating form (F) at pH <4.3 and at pH <2.7 it changes to the
8 fully extended form (E). Whereas on the basic side at pH >8 the N form changes to
9 basic form (B)²⁵. Polyphenols interact with HSA through its binding sites at different
10 domains. HSA has two primary binding sites for various ligands commonly referred as
11 binding site I and II which are located in subdomain IIA and IIIA, respectively¹⁰. HSA
12 binds a variety of molecules, a property that can have profound effects on their
13 pharmacokinetics and pharmacodynamics²⁶. Binding of polyphenols to albumin alters
14 the pattern and volume of distribution, lowers the rate of clearance, and increases the
15 plasma half-life of the drug.

16 The work presented here was focused on dissecting the spectroscopic and
17 thermodynamic basis of HSA-polyphenols interactions investigating the mode and
18 forces responsible for binding. Specifically, the aim of this study was to explore the
19 binding of polyphenols to HSA under normal as well as alkaline conditions. Trp
20 fluorescence quenching was monitored at different temperatures to elucidate the
21 mechanism of TQ binding to HSA. CD and DLS were used to study the effect of TQ
22 binding on the overall conformation of HSA, while ITC was used to determine the
23 thermodynamic of TQ-HSA interaction. We have also monitored the esterase activity

1 and radical scavenging activity of HSA in the presence of TQ. Antioxidant property of
2 TQ plays an important role in various types of diseases and it also dependent on
3 condition such as alkalosis where it's antioxidant activity increases and esterase activity
4 reduces. Therefore, the binding and thermodynamic studies of TQ-HSA interaction
5 shall provide useful information on the structural features that determine the therapeutic
6 efficacy of TQ.

7 **Materials and methods**

8 **Materials**

9 Fatty acid free human serum albumin (A1887), Thymoquinone (274666), Glycine
10 (G8898), *p*-nitrophenyl acetate, 4-*p*-NPA (N8130), 2,2'-Azino-bis (3-ethyl
11 benzothiazoline-6-sulfonic acid) diammonium salt, ABTS (A1888), potassium
12 peroxodisulfate, K₂S₂O₈ (P5592), Trolox (238813) were purchased from Sigma Aldrich
13 and MOPS (134894) buffer was purchased from SRL.

14 **Sample preparation**

15 A stock solution of HSA was made in 20 mM MOPS pH 7.4 and glycine-NaOH pH 9.0
16 buffers and the protein concentrations was determined spectrophotometrically using
17 $E_{280\text{ nm}}^{1\%}$ of 5.30 at 280 nm^{7, 8} on a Perkin-Elmer Lambda 25 spectrophotometer.
18 Buffers used throughout the experiments were filtered by 0.45 μm Millipore Millex-HV
19 PVDF filter and pH was measured using Mettler Toledo (model S20) pH meter. The
20 stock solution of TQ (5mM) was prepared in 10% ethanol and finally adjusted to 1.0 ml
21 by diluting with respective buffers.

22 **UV-visible absorption measurements**

1 UV-visible spectra were recorded between 250 and 350 nm on Perkin-Elmer Lambda
2 25 double beam spectrophotometer attached with Peltier temperature programmer
3 (PTP-1) to maintain temperature at 37 °C throughout the experiments. HSA (6 μM) was
4 titrated by 0-30 μM TQ in a 1 cm path length cuvette of 3 ml. All HSA-TQ absorbance
5 spectra were corrected with respective blank, which consist same concentration of TQ
6 in buffer in the absence of HSA.

7 **Fluorescence quenching measurements**

8 All the fluorescence measurements were carried out on Shimadzu (RF-5301PC)
9 fluorescence spectrophotometer equipped with a constant temperature holder attached
10 with Neslab RTE-110 water bath with an accuracy of ±0.1 °C. Intrinsic fluorescence
11 was measured by exciting HSA (2 μM) at 295 nm and the emission spectrum was
12 measured in the range of 300-450 nm, because tryptophan fluorescence is used as a
13 probe of local environment in a protein for determination of protein structure, dynamics
14 as well as ligand binding. The decrease in fluorescence intensity at particular
15 wavelength was analyzed according to the Stern-Volmer equation 1⁸:

$$\frac{F_o}{F} = K_{sv} [Q] + 1$$

17 (1)

18 where F_o and F were the fluorescence intensities in the absence and presence of
19 quencher (TQ), K_{sv} is the Stern-Volmer quenching constant. Binding constants and
20 binding stoichiometry were obtained from equation 2²⁷:

$$K_{sv} = k_q \cdot \tau_o$$

21 (2)

1 where k_q is the bimolecular rate constant of the quenching reaction and τ_0 is the average
2 integral fluorescence life time of tryptophan which is $\sim 5.78 \times 10^{-9} \text{ s}^{28}$.

$$3 \quad \log\left(\frac{F_0}{F} - 1\right) = \log K_b + n \log[Q] \quad (3)$$

4 where K_b is the binding constant and n is binding stoichiometry.

5 The thermodynamic parameters i.e. change in enthalpy (ΔH°) and change in entropy
6 (ΔS°) were determined after measuring K_b at different temperatures and the results were
7 analyzed according to van't Hoff equation 4:

$$8 \quad \ln K_b = -\frac{\Delta H^\circ}{RT} + \frac{\Delta S^\circ}{R} \quad (4)$$

9 where R is universal gas constant ($1.987 \text{ cal mol}^{-1} \text{ K}^{-1}$).

10 The change in Gibbs free energy (ΔG°) can be further determined from separate terms
11 of enthalpy change (ΔH°) and entropy change (ΔS°) according to the equation 5:

$$12 \quad \Delta G^\circ = \Delta H^\circ - T\Delta S^\circ \quad (5)$$

13 The three-dimensional fluorescence measurement were performed on Hitachi F-4500
14 spectrofluorometer under the following condition: the emission wavelength was
15 recorded between 200 and 600 nm, the initial excitation wavelength was set to 200 nm
16 with increment of 5 nm, the excitation and emission slit widths were fixed at 10 nm²⁹.

17 **Isothermal titration calorimetric measurements (ITC)**

18 The energetics of the binding of TQ to HSA at 37 °C was measured by using a VP-ITC
19 titration microcalorimeter (MicroCal Inc., Northampton, MA). Prior to begin the
20 titration experiment, all samples were degassed on a thermovac. The sample cell loaded
21 with 20 μM HSA dissolved in pH 7.4 and pH 9.0 and reference cell filled with the
22 respective buffer. Multiple injections of 10 μL of TQ solution (3.0 mM) were made into

1 the sample cell containing serum albumin. Each injection was made over 20 s with an
 2 interval of 180 s between successive injections. The reference power and stirring speed
 3 were set at $16 \mu\text{cal s}^{-1}$ and 307 rpm, respectively. Heats of dilution for the ligands were
 4 determined by the control experiments, and these were subtracted from the integrated
 5 data before curve fitting. The first derivative of temperature dependence of enthalpy
 6 change is used for the calculation of experimental heat capacity change calculated from
 7 equation 6³⁰:

$$8 \quad \Delta C_p^{\text{exp}} = \frac{d\Delta H}{dT} \quad (6)$$

9 Temperature dependent van't Hoff enthalpy (ΔH_{vH}) at particular temperature is
 10 calculated by the equation:

$$11 \quad \Delta H_{\text{vH}} = \left[\frac{\left\{ \ln \frac{K(T_2)}{K(T_1)} - \frac{\Delta C_p}{R} \ln \frac{T_2}{T_1} + \frac{\Delta C_p T_1}{R} \left(\frac{1}{T_1} - \frac{1}{T_2} \right) \right\} \times R}{\left(\frac{1}{T_1} - \frac{1}{T_2} \right)} \right] \quad (7)$$

12 where, T_1 and T_2 are the maximum and minimum experimental temperature, $K(T_1)$ and
 13 $K(T_2)$ are the values of binding constant at respective temperatures.

14 **Circular dichroism (CD) measurements**

15 CD measurements were carried out with a Jasco spectropolarimeter (J-815) attached
 16 with a Peltier-type temperature controller. The instrument was calibrated with D-10-
 17 camphorsulfonic acid. All The CD measurements were carried at pH 7.4 and pH 9.0 at
 18 physiological temperature $37 \text{ }^\circ\text{C}$. Spectra were collected with a scan speed of 50
 19 nm/min, data pitch 0.1 nm and a response time of 2 s. Each spectrum was the average
 20 of 2 scans. Far-UV CD spectra (190-250 nm) were taken at TQ concentrations from 0-

1 50 μM with protein concentrations of 2 μM and 0.1cm path length cells. The results
 2 were expressed as mean residue ellipticity (MRE) in degree $\text{cm}^2 \text{dmol}^{-1}$, which is
 3 defined as:

$$4 \quad \text{MRE} = \frac{\theta_{\text{obs}} (m \text{ deg})}{10 \times n \times C \times l} \quad (8)$$

5 where θ_{obs} is the observed ellipticity in degrees, C is the molar concentration of HSA, n
 6 is the number of amino acid residues ($585-1=584$) and l is the pathlength of cuvette in
 7 centimeter. Helical content of HSA was calculated from the MRE values at 222 nm
 8 using the following equation as described by Chen *et al.*³¹:

$$9 \quad \% \alpha\text{-helix} = \left(\frac{\text{MRE}_{222\text{nm}} - 2,340}{30,300} \right) \times 100 \quad (9)$$

10 The thermal denaturation experiments were carried between 25-90 $^{\circ}\text{C}$ with 1 $^{\circ}\text{C min}^{-1}$
 11 temperature slope probed by far-UV CD at 222 nm. The curves were normalized,
 12 assuming a linear temperature dependence of the base lines of native and denatured
 13 states.

14 **Data analysis of thermal denaturation**

15 Thermal denaturation data from CD spectroscopy were analyzed on the basis of two-
 16 state unfolding model. For a single step unfolding process, $\text{N} \rightleftharpoons \text{U}$, where N is the native
 17 state and U is the unfolded state, the equilibrium constant K_u is:

$$18 \quad K_u = \frac{f_u}{f_n} \quad (10)$$

19 with f_u and f_n being the molar fraction of U and N, respectively.

$$20 \quad f_d = \frac{(Y_{\text{obs}} - Y_n)}{(Y_u - Y_n)} \quad (11)$$

1 where Y_{obs} , Y_{n} and Y_{u} represent the observed property, the property of the native state,
2 and the property of unfolded state, respectively.

3 **Dynamic light scattering measurements**

4 DLS measurements were carried out at 830 nm by using DynaPro-TC-04 dynamic light
5 scattering equipment (Protein Solutions, Wyatt Technology, Santa Barbara, CA)
6 equipped with a temperature-controlled micro sampler. HSA (30 μM) was incubated
7 with the different concentration of TQ for 8 h, before scanning the samples were spun
8 at 10,000 rpm for 10 min and were filtered serially through 0.22 and 0.02 μm Whatman
9 syringe filters directly into a 12 μl quartz cuvette. For each experiment, 20
10 measurements were taken. Mean hydrodynamic radius (R_{h}) and polydispersity were
11 analyzed using Dynamics 6.10.0.10 software at optimized resolution. The R_{h} was
12 estimated on the basis of an autocorrelation analysis of scattered light intensity data
13 based on translation diffusion coefficient by Stoke's-Einstein relationship-

$$14 \quad R_{\text{h}} = \frac{kT}{6\pi\eta D} \quad (12)$$

15 where R_{h} is the hydrodynamic radius, k is Boltzmann constant, T is the absolute
16 temperature, η is the viscosity of water and D is the diffusion coefficient³².

17 **Tryptophan fluorescence resonance energy transfer (FRET) to TQ**

18 The fluorescence spectra of HSA (2 μM) and absorption spectra of TQ (2 μM) between
19 300 to 400 nm were scanned in similar way as given in method sections 'Fluorescence
20 quenching' and 'UV-visible' experiments at 37 $^{\circ}\text{C}$. If the emission spectrum of donor
21 (Trp214) significantly overlaps with the absorption spectrum of acceptor (TQ), these
22 donor-acceptor pairs will be considered in Förster distance and then we could ascertain
23 the possibility of energy transfer³³. Therefore, the degree of energy transfer depends

1 upon the area of overlap and the distance between these donor-acceptor molecules. The
 2 efficiency of energy transfer (E) is calculated using the following equation ³⁴:

$$3 \quad E_{\text{FRET}} = \left(1 - \frac{F}{F_0}\right) = \frac{R_0^6}{R_0^6 + r^6} \quad (13)$$

4 where F_0 and F were the fluorescence intensities of HSA in absence and presence of TQ
 5 respectively; r is the distance between donor and acceptor and R_0 is the critical distance
 6 at which transfer efficiency equals to 50% which can be calculated from the following
 7 equation:

$$8 \quad R_0^6 = 8.79 \times 10^{-25} K^2 n^{-4} \phi J \quad (14)$$

9 where K^2 is the orientation factor related to the geometry of the donor and acceptor of
 10 dipoles, n is the refractive index of the medium, ϕ is the fluorescence quantum yield of
 11 the donor in absence of acceptor; and J expresses the degree of spectral overlap
 12 between the donor emission and the acceptor absorption which can be evaluated by
 13 integrating the overlap spectral area in between 300 to 400 nm from following
 14 equation:

$$15 \quad J = \frac{\int_0^{\infty} F(\lambda) \varepsilon(\lambda) \lambda^4 d\lambda}{\int_0^{\infty} F(\lambda) d\lambda} \quad (15)$$

16 where $F(\lambda)$ is the fluorescence intensity of the donor at wavelength range λ which is
 17 dimensionless, and $\varepsilon(\lambda)$ is the molar absorptivity (extinction coefficient) of the acceptor
 18 at wavelength λ in $M^{-1} \text{ cm}^{-1}$. In the present study, K^2 , n and ϕ were taken as 2/3, 1.336
 19 and 0.118, respectively ³⁵.

20 **Molecular docking parameters**

1 The three dimensional X-ray crystal structure of HSA (PDB ID: 1AO6, resolution 2.5
2 Å) was downloaded from the RCSB Protein Data Bank. The three dimensional
3 structure of TQ was retrieved from pubchem [CID: 10281]. We performed docking
4 studies using docking program AutoDock version 4.0^{36, 37}. AutoDock works on
5 Lamarkian genetic algorithm and calculate all possible conformations of the ligand that
6 binds to the protein. Polar hydrogen atoms, Kollman charges were merged to the
7 protein and Gasteiger charges were added to the ligands using graphical user interface
8 program AutoDock Tools (ADT) and then prepared file was saved in PDBQT format.
9 For the preparation of the grid map using a grid box Auto-Grid was used. Size of grid
10 was set to 70 Å × 70 Å × 70 Å xyz points with spacing of 0.375 Å, which covers all the
11 available active site residues. To encompass two binding sites (subdomain IIA and
12 IIIA, respectively) during the docking process, the two different grid centers along the
13 x-, y-, z-axes were set for subdomain IIA and for subdomain IIIA, respectively. To
14 achieve our goal the complex showing lowest binding energy with best fitness score
15 was used. For visualization purpose we used Pymol version 1.3 and chimera version
16 1.8³⁸.

17 **Enzyme activation kinetics by esterase activity (*Determination of esterase-like***
18 ***activity*):**

19 The reaction of *p*-nitrophenyl acetate with HSA was followed spectrophotometrically
20 by monitoring the appearance of *p*-nitrophenol³⁹ at 405 nm for time duration of 2 min
21 on Perkin-Elmer Lambda 25 double beam spectrophotometer attached with Peltier
22 temperature programmer (PTP-1) to maintain temperature at 25 °C throughout the
23 experiments. The reaction mixtures contained 5 μM *p*-nitrophenyl acetate and 5 μM

1 protein in 20 mM MOPS (pH 7.4) and 20 mM glycine-NaOH (pH 9.0) buffers. The
2 Michaelis-Menten equation was used to get the rectangular hyperbolic pattern of a
3 typical enzyme-substrate reaction-

$$4 \quad v_o = \frac{V_{\max} \cdot [S]}{K_m + [S]} \quad (16)$$

5 where V_o and V_{\max} is the initial and maximum velocity respectively, $[S]$ is the substrate
6 concentration, K_m is the Michaelis-Menton constant. The reciprocal of catalytic
7 velocity was plotted against the reciprocal of substrate concentration at a constant
8 activator concentration according to the equation 18 (Lineweaver-Burk plot):

$$9 \quad \frac{1}{V_o} = \frac{K_m}{V_{\max} + [S]} + \frac{1}{V_{\max}} \quad (18)$$

10 **Antioxidant or Free radical scavenging activity (a decolorization assay):**

11 The antioxidant activity experiments were performed on the Perkin-Elmer Lambda 25
12 double beam spectrophotometer attached with Peltier temperature programmer (PTP-1)
13 to maintain temperature at 37 °C throughout the experiments. The TEAC assay was
14 performed as described by Re *et al.*⁴⁰ with minor modifications. ABTS was dissolved
15 in respective buffers (pH 7.4 and pH 9.0) to a 7 mM concentration. ABTS radical
16 cation ($ABTS^{+\cdot}$) was produced by reacting ABTS stock solution with 2.45 mM
17 potassium persulfate (final concentration) and allowing the mixture to stand in the dark
18 at room temperature for 12-16 h before use. Because ABTS and potassium persulfate
19 react stoichiometrically at a ratio of 1:0.5, this will result in incomplete oxidation of the
20 ABTS. Oxidation of the ABTS commenced immediately, but the absorbance was not
21 maximal and stable until more than 6 h. The radical was stable in this form for more
22 than two days when stored in dark condition at room temperature. For the study of

1 phenolic compounds, the ABTS^{•+} solution was diluted with respective buffers (pH 7.4
2 and pH 9.0) to an absorbance of 0.71 (± 0.02) at 734 nm and equilibrated at 37 °C. After
3 addition of antioxidant the absorbance was measured at 734 nm at 37 °C exactly 30 min
4 after initial mixing. Appropriate solvent blanks were run in each assay and subtracted,
5 respectively. All determinations were carried out at least three times, and in triplicate,
6 on each occasion and at each separate concentration of the standard and samples.

7 **Results and discussion**

8 **UV-visible absorption studies**

9 Ultraviolet/visible absorption spectroscopy is a powerful tool for steady-state studies of
10 protein-ligand interaction. In proteins, we distinguish different internal chromophores
11 that give rise to electronic absorption bands. From Fig. 1 we can see that the absorption
12 peak of HSA centers at ~280 nm mainly due to absorption of tryptophan residue.
13 However, after addition of the TQ, the maximal absorption peak as well as absorption
14 intensity of HSA is slightly affected. We observed that upon increasing the
15 concentration of TQ, the conformation of HSA was slightly affected. It was evident
16 from the disrupted absorption spectra of HSA around 280 nm (corresponding to Trp
17 residue) and 256 nm (corresponding to transition region of disulphide bond and Phe
18 residues absorption) in the presence of TQ.

19 **Tryptophan fluorescence quenching by TQ**

20 To avoid the effect of phenylalanine, we explored Trp fluorescence quenching
21 experiments to determine the interaction of TQ with 'N' and 'B' isoforms (at pH 7.4
22 and pH 9.0, respectively) of HSA at 37 °C. We observed a strong fluorescence peak of
23 HSA around 340 nm when excited at 295 nm in the absence of TQ. The fluorescence of

1 HSA was quenched in the presence of increasing concentrations of TQ, clearly
2 indicating an interaction between TQ and HSA (Supplementary Fig. S1). The intensity
3 of tryptophan fluorescence emission decreases continuously and gets saturated at higher
4 TQ concentrations, proving that TQ binding sites on HSA was fully occupied. The
5 decrease in fluorescence intensity upon addition of polyphenols was analyzed
6 according to the Stern-Volmer equation 1. There is a linear dependence between F_0/F
7 and molar concentration of the TQ (1:1). The qualitative emission spectral features
8 were slightly affected upon interaction of TQ to HSA which suggests about the minor
9 ligand-induced conformational changes in the protein occurs due to increase in
10 molecular closeness of TQ. The same experimental procedures were also followed at
11 15, 25 and 45 °C where we found that upon increasing the temperature, the quenching
12 also decreases, or in other words, the extent of lowering in fluorescence emission was
13 higher at lower temperatures (Fig. 2 A-I and B-II). The K_{sv} values for TQ at different
14 temperature as well as at different pH are given in the Table 1.

15 **Determination of binding constant and binding stoichiometry**

16 The binding constant (K_b) and the number of binding sites (n) can be calculated using
17 the equation 2. A plot of $\log [(F_0/F) - 1]$ vs $\log [TQ]$ gives a straight line, whose slope
18 equals to binding stoichiometry (n) and the intercept on y-axis equals to binding
19 constant (K_b), respectively (Fig. 2A-II and B-II). The values of K_b and n at 15, 25, 37
20 and 45 °C are listed in Table 1. For TQ, the values of K_b and n at pH 7.4 and 9.0 were
21 calculated at different temperatures as well as in presence of salt (NaCl). The data
22 shows that K_b decreases on increasing the temperature in both 'N' and 'B' isoforms but
23 these values are greater for 'N' ($1.63 \times 10^4 \text{ M}^{-1}$) than the 'B' ($0.28 \times 10^4 \text{ M}^{-1}$) form at

1 physiological temperature. It implies that under basic conditions the binding capacity of
2 TQ reduces up to ~6 times than that under neutral (physiological) conditions.
3 Conclusively, it shows that pH induced conformational change in the protein affects the
4 mode and mechanism of quenching and hence TQ binding to the HSA molecules.
5 Moreover, in the presence of NaCl, the extent of binding was not significantly changed
6 thus giving the clues that the electrostatic force doesn't play any role in TQ-HSA
7 interactions.

8 **Mechanism of HSA-TQ interaction**

9 Fluorescence quenching can be either dynamic or static in nature. To know about the
10 quenching mechanism of HSA by TQ, the values of k_q obtained from equation 3 was
11 closely observed and found that it was of the order of 10^{12} , which was 100 times higher
12 than the maximum scatter collision quenching constant of various quenchers with
13 biopolymers ($2 \times 10^{10} \text{ M}^{-1} \text{ s}^{-1}$)⁴¹. This shows that quenching is not initiated by
14 dynamic diffusion but occurs by formation of a strong ground state complex between
15 HSA and TQ. Further, the temperature dependency of K_{sv} was studied and we observed
16 that the slopes (K_{sv} values) decreased with increase in temperature, further confirming
17 that the binding of TQ to HSA was due to complex formation (static quenching). In
18 static quenching, K_{sv} decreases due to the formation of complex between ligand and
19 protein, which undergoes dissociation on increasing temperature²⁹.

20 **Thermodynamics of HSA-TQ interaction**

21 According to the binding constants of TQ to HSA at all the four temperatures, the
22 thermodynamic parameters were determined from linear van't Hoff plot (equation 4)
23 and the observed data are shown in Table 1 and supplementary Fig S2. For the

1 determination of enthalpy-entropy relation in protein-ligand interaction we considered
2 only three temperatures *viz.* 15, 25 and 37 °C (NOT 42 °C) to ensure that the integrity
3 of protein conformation was not affect, otherwise it would to lead false interpretation of
4 thermodynamic parameters for the interaction studies. It is very well documented that at
5 42 °C, the domain III of HSA starts to melt, hence, major structural changes occurs
6 beyond this temperature. But we had included the data of 45 °C to assumed the
7 property of protein unchanged ²⁷. In other words, obtained enthalpy-entropy changes
8 are mainly caused by the binding of the TQ molecule to HSA. The negative values of
9 ΔG° manifested in each condition suggest that the interaction was spontaneous. ΔH°
10 and ΔS° for the complex formation between TQ and HSA were found to be -5.10 kcal
11 mol^{-1} and 0.80, 0.83, 0.87 and 0.89 $\text{kcal mol}^{-1} \text{K}^{-1}$, respectively at 15, 25, 37 and 45 °C
12 at pH 7.4 and a similar pattern was also obtained at pH 9.0. Thus, the formation of TQ-
13 HSA complexation is an exothermic reaction accompanied by positive ΔS° value. The
14 role of bound water to the protein molecule in or near the binding pockets may be
15 disturbed as a positive $T\Delta S^\circ$ value is a strong indication that water molecules have been
16 excluded from the binding site interface. From the point of view of water structure,
17 these thermodynamic signatures of protein-ligand interactions impersonate the type of
18 forces responsible for ligand association. A positive ΔS° value is frequently taken as a
19 typical evidence for hydrophobic interaction whereas a negative ΔH° is taken for
20 hydrogen binding ⁴³. Therefore, binding of TQ to HSA might involve H-bonding as
21 well as hydrophobic interaction as evidenced by the above thermodynamic signatures
22 (Supplementary Fig S2). Furthermore, it was found that the major contribution to ΔG°
23 arises from the ΔH° rather than from ΔS° , so binding process was enthalpy driven.

1 **Isothermal titration calorimetric measurements**

2 The associated thermodynamic and binding parameters were further investigated
3 through ITC measurements. Representative calorimetric measurements to determine the
4 mode of binding of TQ with HSA isoforms at 37 °C are shown in Fig. 3. In the ITC
5 profiles, the lower panel shows the plot of heat liberated per injection as a function of
6 molar ratio of the drug to the protein and upper panel, each peak represents the binding
7 isotherm of a single injection of the drug into the protein solution. The titration of TQ
8 to HSA shows negative heat deflection indicating that the reactions were mainly
9 exothermic. The association constant (K_a) and enthalpy change (ΔH°) were directly
10 obtained after the best fitting for the integrated heats was obtained using single set of
11 binding model with lowest χ^2 value. The Gibbs free energy and entropy changes were
12 calculated from equations 6 and 7, respectively and obtained thermodynamic or binding
13 parameters are summarized in Table 1. The binding of TQ shows exothermic process
14 that are the characteristics of hydrogen bond and conformational changes⁴⁴ and the
15 values of binding constant were varying in the range of 10^3 to 10^4 . Moreover, the
16 negative value of ΔG° suggests that the TQ-HSA complex formation was spontaneous
17 at both pH values (pH7.4 and pH 9.0). The negative values of ΔH° and positive value
18 of ΔS° values advocate that the involvement of hydrogen bond and hydrophobic
19 interaction in the formation of the protein-TQ complex⁴⁵, which indicates the
20 occurrence of enthalpy-entropy compensation effect in which enthalpy loss due to the
21 deformation of H-bond is counter balanced by entropic penalty due to the burial of
22 involved groups. This effect is common in protein-ligand interactions⁴⁶.

23 **Circular dichroism measurement**

1 It is possible to estimate the contents of secondary structure of protein using far-UV CD
2 spectra (190-250 nm). A positive peak near 195 nm and two negative peaks near 208
3 and 222 nm is characteristic feature of α -helical protein. The far-UV CD studies were
4 performed on the protein and protein-TQ complexes in order to investigate the
5 possibility of any structural change of the protein upon complexation with the TQ. Fig
6 4-I shows that the CD spectra of HSA with various TQ concentrations at pH 7.4 and
7 9.0. From Fig. 4-IA (pH 7.4) and 4-IB (pH 9.0) the spectra of HSA in the absence and
8 presence of TQ, as the TQ concentration increases a notable spectral rearrangement
9 occurs in HSA with increase in major minima (208 nm) as well as slight changes in the
10 shape of spectra due to intramolecular H-bonding rearrangement as justified by
11 fluorescence quenching experiments. The TQ induced alterations in secondary
12 structures of HSA were quantified by Chen *et al.* method³¹, and the calculated values
13 are summarized in Table 2. In the presence of TQ, a significant increase in the α -helical
14 content of both HSA isoforms was observed. Using equation 9, the α -helical content in
15 'N' isoform of HSA was calculated. It increased from 4% and 9% while in case of 'B'
16 isoform of HSA it increased from 9% and 18% as compared to native structure,
17 correspondingly. Overall, the 'B' isoform of HSA is more stable in the presence of TQ.

18 **Thermal stability of albumin was enhanced by TQ**

19 The existence of intermediates in the thermal unfolding pathway of a protein can also
20 be evidenced by observing the changes in its secondary structure. Fig. 4-II shows the
21 change in the ellipticity at 222 nm of the HSA:TQ at molar ratios 1:0, 1:5 and 1:25,
22 respectively as obtained from CD experiments. The mid-point temperature (T_m) was
23 determined by fitting the ellipticity values in to a two-state folding-unfolding model

1 equation 10 and 11. This shows that the protein loses a considerable fraction of its
2 secondary structure during thermal denaturation. The decrease in ellipticity at 222 nm
3 of HSA is shown as a function of temperature and the denaturation profile is found to
4 be consistent with the earlier reports⁴⁷. It is noted that the presence of intermediate
5 unfolded states in the thermal denaturation of bovine serum albumin (BSA), which is
6 structurally similar to HSA, has already been indicated by calorimetric studies⁴⁸. The
7 CD thermal profiles, including the 1:25 molar ratio of HSA:TQ showed more thermal
8 stability, indicating that the protein is more stable in the presence of TQ as compared to
9 the native condition. Thus, the higher stability of HSA in the presence of 1:25 molar
10 ratio corresponds to increase in the secondary structure. The obtained T_m values of TQ-
11 bound HSA are significantly higher than the native one (Table 2). Denaturation of HSA
12 at high temperature occurs by weakening of hydrophobic as well as polar interactions,
13 which may also facilitate the TQ binding property of HSA. Here, enhancement in
14 thermal stability is also implied by better interaction of TQ at high temperature which
15 induces to more helical structure formation in unordered protein segments of 'B'
16 isoform as compare to 'N' isoform of HSA.

17 **Dynamic light scattering studies**

18 Unfolding of a protein is usually marked by a change in the secondary and globular
19 structure of the protein. The change in the globular structure of a protein can be studied
20 by DLS measurements. It is clear from the above findings that the interaction of TQ
21 with HSA causes conformational changes. So, we decided to measure the molecular
22 sizes of HSA in the absence and presence of TQ by determining the hydrodynamic radii
23 using DLS. The Fig. 5-I & 5-II shows that the change in the globular structure of the

1 protein at 25 °C. The hydrodynamic radii (R_h) of native HSA and HSA in the presence
2 of TQ were calculated and values are shown in Table 3. The R_h values of native HSA
3 were 4.0 nm and 3.6 nm at pH 7.4 and 9.0, respectively. These results are in excellent
4 agreement with previous observations at pH 7.4 and pH 9.0, respectively ⁴⁹. The R_h
5 values of HSA complexed with TQ were higher than the native one. The increase in
6 hydrodynamic radii upon ligand binding may be due to the “expansion of domains”
7 which may lead to an increase in the molecular volume as a result of conformational
8 changes. Similar results were also observed previously in the presence of atropine
9 (4.1%), propranolol (11.1%), clonidine (14.4%), phenylephrine (16.6%) and carbachol
10 (15.5%) ⁵⁰. The lower values of polydispersity (< 20) were indicative of homogenous
11 species in the solution. Fig. 5-II shows the characteristic examples of the dependencies
12 of globule size and compressibility upon the HSA:drug molar ratios. The principal
13 structural rearrangements were displayed at each HSA:drug molar ratios and it
14 increased with an increase in HSA:drug ratio. We observed that at extremely higher
15 molar ratio of HSA:drug (1:25), the hydrodynamic radii were either slightly changed or
16 remain unaffected (Fig. 5-II). It suggested that the structural changes in HSA occurred
17 only by the molecules which were bound to the protein and affected its secondary
18 structures near the binding site ⁵¹.

19 **Energy transfer between TQ and HSA**

20 In order to estimate the binding of TQ to the model transporter protein HSA, we have
21 also explored the possibility of energy transfer between donor to acceptor using
22 Förster’s resonance energy transfer (FRET) method. In Fig. 6, the emission spectrum
23 from the single tryptophan (Trp214) of HSA and the absorption spectrum of TQ are

1 shown. According to FRET theory as describe in the method section, efficiency of
2 energy transfer (E_{FRET}), spectral overlap (J), Förster's distance (R_0) of the donor
3 (Trp214), and r value were derived from the overlaid spectra and the value of energy
4 transfer between TQ and HSA was calculated from the equations 13-15. At pH 7.4, the
5 energy was efficiently transferred from Trp214 of HSA to the bound TQ as indicated
6 by a large spectral overlap between the emission spectra of Trp214 and the absorption
7 spectrum of TQ. Hence, the probability of TQ binding was stronger with the 'N' isomer
8 of HSA at pH 7.4. Further, it is evident from the Fig. 6B that the spectral overlap of the
9 HSA-TQ system was significantly lower at pH 9.0 due to minimum contribution from
10 the Trp214. We calculated the energy transfer parameters and found that $E_{\text{FRET}} =$
11 0.3048 , $J = 3.24 \times 10^{-14} \text{ cm}^3 \text{ M}^{-1}$, $R_0 = 2.981 \text{ nm}$, $r = 3.42 \text{ nm}$ for HSA at pH 7.4 and
12 $E_{\text{FRET}} = 0.1400$, $J = 2.72 \times 10^{-15} \text{ cm}^3 \text{ M}^{-1}$, $R_0 = 1.97 \text{ nm}$, $r = 2.66 \text{ nm}$ for HSA at pH 9.0,
13 respectively (Table 4). The average distance between the donor and acceptor
14 fluorophores was on the 2-8 nm scale and $0.5R_0 < r < 1.5R_0$. In our study, the donor to
15 acceptor distance was less than 8 nm, indicating that the energy transfer from HSA to
16 TQ occurred with high probability. These results were also in accordance with a static
17 quenching mechanism.

18 **Three-dimensional conformational investigation of TQ binding with HSA**

19 Three-dimensional fluorescence spectroscopy is a new analytical technique that is
20 applied to investigate the conformational changes of proteins. The excitation and
21 emission wavelength of the fluorescence intensity can be used as the axes rendering the
22 investigation of the characteristic conformational changes of proteins more scientific
23 and credible ²⁹. The maximum fluorescence emission wavelength of amino acid

1 residues in a protein is related to the polarity of the environment. Experiments have
2 suggested that the fluorescence emission spectrum wavelength and the synchronous
3 fluorescence spectrum wavelength of HSA in the absence and presence of drugs show
4 distinct differences and sharp changes, which provide relative information on the
5 configuration of the protein⁵². The three-dimensional spectra and contour maps of HSA
6 and HSA-TQ complexes are presented in Fig. 7 and supplementary Fig. S3 and the
7 obtain values are listed in supplementary Table T-1. In the figure of three-dimensional
8 spectra, two characteristic fluorescence peaks of HSA (peak 1 and peak 2) were clearly
9 observed, while peak 3 and peak 4 represents Rayleigh scattering peak ($\lambda_{\text{ex}} = \lambda_{\text{em}}$) and
10 second-order scattering peak ($\lambda_{\text{em}} = 2\lambda_{\text{ex}}$)^{29, 52}, respectively. The peak 1 represents
11 fluorescence arising mainly from tryptophan and tyrosine (negligible contribution of
12 phenylalanine fluorescence) when the protein is excited at 280 nm. On the other hand,
13 peak 2 is the characteristic fluorescence peak representing polypeptide backbone
14 structure. In our study, the decrease in the intensities of peaks 1 and 2 clearly indicated
15 that the fluorescence of HSA was quenched as a result of TQ binding and the
16 conformation of the protein was also altered as a result of it.

17 **Molecular docking**

18 Main aim of the study was to presumptive binding site of TQ in HSA as reported earlier
19 by G. Lupidi *et al.*¹³. We used X-ray structure of HSA with high resolution (PDB ID:
20 1AO6, res. 2.5 Å) as a template and the prediction of binding mode of TQ was done
21 using AutoDock software package. To comprise the subdomain IIA and IIIA of HSA,
22 the two regions of interest used for molecular docking were defined to determine the
23 binding residues and their positions and their energy score was compared. The docking

1 results showed that TQ binds to HSA within the binding pocket of subdomain IIA with
2 an estimated docking energy of about $-5.83 \text{ kcal mol}^{-1}$, while for the second binding site
3 subdomain IIIA the free energy of binding was found to be $-5.62 \text{ kcal mol}^{-1}$.

4 Therefore we can argue that TQ has a better binding preference for the drug binding
5 site I (subdomain IIA) of HSA. This result is in agreement with earlier published data,
6 as it is reported that quinone-related derivatives bind to subdomain IIA of HSA. The
7 binding of TQ to subdomain IIA of HSA was also confirmed by the drug-displacement
8 experiments^{54, 55}. This binding site for TQ at subdomain IIA was located
9 predominantly in a hydrophobic cleft walled by the amino acid residues Tyr150,
10 Leu199, Trp214, Leu219, Arg222, Leu238, Arg257, Leu260, Ala261, Ile264, Ser287,
11 Ile290, and Ala291 (as shown in Fig.8A). One of the oxygen from TQ was interacting
12 with Tyr150 through hydrogen bonding, and its methyl group was found to interact
13 with Trp214 through hydrophobic interactions (Fig. 8B).

14 **Esterase-like activity of HSA-isoforms in presence of TQ**

15 HSA has an esterase-like activity for the deglucuronidation of acyl-glucuronide of
16 fenoprofen, etodolac, ketoprofen and gemfibrozil⁵⁶⁻⁵⁹. The double-reciprocal plots for
17 substrates were characterized by a family of linear, nonparallel lines that converged to
18 the left of the y-axis (Supplementary Fig. S4). In presence of TQ, the K_m increased at
19 pH 7.4 from $6.66 \times 10^{-6} \text{ M}$ to $9.37 \times 10^{-6} \text{ M}$. The higher value of K_m obtained for the
20 HSA incubated at pH 7.4 in the presence of TQ showed a lower substrate affinity for
21 the substrate. The incubated enzyme besides showing higher K_m for substrate also
22 showed a higher k_{cat} value yielding overall a decrement in catalytic efficiency (k_{cat}/K_m)
23 relative to the HSA in the absence of TQ. Altogether, our results indicated that addition

1 of TQ alters both K_m and V_{max} values of HSA. Increase in K_m and V_{max} indicated that
2 the esterase activity of HSA was inhibited in a competitive manner because TQ was
3 directly competing with the substrate for a fixed number of active sites on enzymes.
4 The large increase in K_m upon the binding of TQ indicated changes in the tertiary
5 structure of HSA that might lead to steric effects resulting from limitation of the
6 accessibility of substrate to the active site. The catalytic efficiency value, which is the
7 ratio of k_{cat} over K_m was also different for free HSA and HSA-TQ complex. As shown
8 in Table 5, the catalytic efficiency of HSA-TQ was lower than the free enzyme
9 indicating that the enzyme was poorer on the substrate in the presence of TQ.

10 We have obtained opposite pattern of K_m and V_{max} at pH 9.0, decrease in K_m from
11 8.55×10^{-5} M to 4.09×10^{-5} M and V_{max} 6.70×10^{-7} to 5.12×10^{-7} M/min revealed that
12 HSA in the presence of TQ at pH 9.0 had an improved affinity and tighter substrate
13 binding capability as compared to that at pH 7.4 (Table 5). The second order rate
14 constant k_{cat}/K_m ratio indicates the catalytic efficiency and kinetic perfection of the
15 enzyme in transforming substrates. The higher the k_{cat}/K_m ratio, the better the enzyme
16 works on that substrate. A comparison of k_{cat}/K_m ratio for the same enzyme with
17 substrates in different conditions is widely used as a measure of enzyme effectiveness.

18 TQ induced the catalytic activation of HSA at pH 9.0 and allowed the reaction to
19 approach the limit of maximum diffusion just like in an ideal enzyme (acetyl
20 cholinesterase) where every interaction with substrate yields a product and for these
21 enzymes, from the diffusion theory, the value of k_{cat}/K_m ranges 6×10^9 - 6×10^{10} $M^{-1} min^{-1}$.
22 Our enzyme kinetics results suggested that the TQ acts as an activator of the esterase
23 activity of HSA in alkaline conditions. The k_{cat} values were strikingly dependent on pH

1 and showed that the susceptibility of the active sites to nucleophilic attack increases
2 with pH. It has been reported that pH dependent conformational changes ('N' \leftrightarrow 'B'
3 transition) occur in albumin when going from neutral to slightly alkaline pH ²⁵.
4 Therefore, alteration in nucleophilic attack in active sites and in the affinity to *p*-NPA
5 could be due, totally, or partly, to changes in the tertiary structure of albumin, which
6 convey the pH-dependent N-B transition. From all of our experiments dealing with the
7 secondary and tertiary structure of HSA in the presence of TQ molecules, it becomes
8 apparent that upon interaction between TQ and HSA, the affinity of the protein for its
9 substrate is enhanced in alkaline condition.

10 **Antioxidant or Radical scavenging activity of HSA in presence of TQ**

11 TQ has several important functional properties, out of them we have evaluated the
12 free radical scavenging activity because of its deleterious job in the food and biological
13 systems ⁶⁰. Some of its properties were previously demonstrated by several
14 pharmacological studies as membrane lipid peroxidation, reduction of eicosanoid
15 generation ⁶¹, anti-inflammatory and analgesic ^{2, 62}, protection of body organs against
16 oxidative damage induced by various type free radical generating agents ⁶³⁻⁶⁵. Oral
17 intake of TQ is capable of protecting numerous organs against oxidative damage
18 induced by free radical-generating agents including doxorubicin-induced cardiotoxicity
19 ^{66, 67}. TQ act as scavenger of superoxide, hydroxyl radical and singlet molecular oxygen
20 ⁶⁸. HSA itself have a very good antioxidant activity that plays an important role in
21 human health. In alkaline condition, antioxidant property of HSA increases due to its
22 conformational change and the activation of antioxidant activity is also thiol-dependent
23 ⁶⁹. The carboxyl group modification of HSA causes approximately 40-fold increase in

1 the antioxidant activity. These chemical modification studies indicate that the addition
2 to functional cysteine(s) or cationic amino acid residues such as arginine, histidine and
3 lysine involve in antioxidant reactions. These results recommend that the
4 activation of thiol-dependent antioxidant activity of HSA at alkaline pH is due to
5 the conformational change which was favorable for the functional cysteine(s)-mediated
6 catalysis. HSA shows specific antioxidant property is also due to its multiple ligand-
7 binding and free radical-trapping properties and are directly connected to the
8 conformational change in structure and the redox state of molecule^{70, 71}. Currently
9 various methods are used to described the antioxidant activity of plant derived phenolic
10 compounds. These chemical assays are based on the ability to scavenge the free radical
11 by various radical generating system and method for decolorization. ABTS^{•+} radical
12 scavenging method is most appropriate format for decolorization assay and very
13 common spectrophotometric procedure to determine the antioxidant capacity of plant
14 derived components due to its sensitive, simple, rapid and reproducible procedure⁷².
15 Biochemical assay are based on the scavenging ability of synthetic free radicals which
16 are generated by different radical-generating systems. Free radicals are generating prior
17 to reactions that involve in the production of blue/green ABTS^{•+} chromophores that was
18 formed due to reaction between ABTS and potassium persulphate.



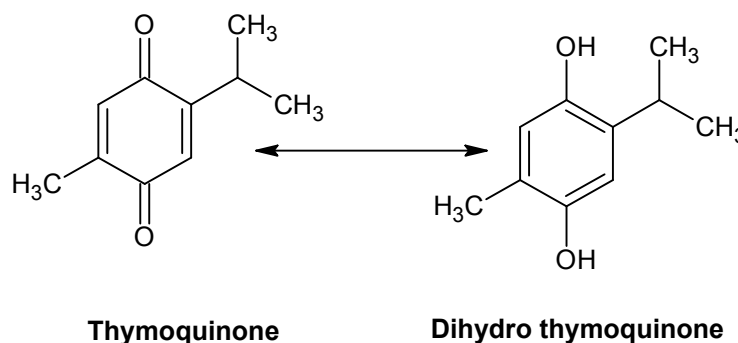
20 The extent of inhibition of the absorbance of the ABTS^{•+} is plotted as a function of
21 concentration in order to determine the TEAC, that can be assessed as a function of
22 time. The dose-response curve obtained by analysis of a range of concentrations of
23 antioxidant compounds, was plotted as the percentage inhibition of the absorbance of

1 the ABTS^{•+} solution as a function of concentration of antioxidant (Fig. 9A). Trolox and
2 BHA were used as standard reference compounds (Fig. 9B). To calculate the TEAC,
3 the gradient of the plot of the percentage inhibition of absorbance vs. concentration plot
4 for the antioxidant in question is divided by the gradient of the plot for Trolox and
5 BHA. The scavenging capability of ABTS^{•+} radical was calculated using the following
6 equation:

$$7 \quad ABTS^{\bullet+} \text{ scavenging effect (\%)} = \left(1 - \frac{As}{Ac}\right) \times 100 \quad (19)$$

8 where, Ac is the initial concentration of the ABTS^{•+} and As is absorbance of the
9 remaining concentration of ABTS^{•+} in the presence of TQ⁷³.

10



12

13 This gives the TEAC at the specific time point and the calculated results for the
14 flavonoids are given in supplementary Table T-2. All the tested compounds exhibited
15 admirable radical cation scavenging activity. As seen in Fig. 9C, TQ had effective
16 radical scavenging activity in a concentration-dependent manner (16.42-164.2 µg/ml).
17 TQ undergoes reduction process and gets converted into its more anti-oxidative form
18 i.e. dihydrothymoquinone (DHTQ). TQ and DHTQ inhibited non-enzymatic process in
liver that was also dose dependent⁶⁷. There was a significant increase in the overall

1 concentration of ABTS^{•+} due to the scavenging capacity of TQ concentrations. Also,
2 the scavenging effect of TQ and standards, on the ABTS^{•+} decreased in that order: at
3 pH 7.4 HSA-TQ > HSA (100 μM) > TQ (2500 μM) > trolox (100 μM), which were
4 81.39%, 50.37%, 47.45% and 43.76% , and at pH 9.0 HSA-TQ > HSA (100 μM) > TQ
5 (2500 μM) > trolox (100 μM), which were 100%, 99.97%, 96.19% and 88.39% at the
6 concentration of 100 μL/ml respectively.

8 **Conclusion**

9 In the present study, we evaluated the binding properties of ‘N’ and ‘B’ isoform of
10 HSA (at pH 7.4 and pH 9.0, respectively) with TQ, an important constituent of *Nigella*
11 *sativa*. The binding affinity and thermodynamics parameters were higher for ‘N’
12 isoform as compared to ‘B’ isoform of HSA. The interaction of TQ with HSA was
13 favored by H-bonding and hydrophobic interactions. The molecular size and thermal
14 stability of HSA were increased in the presence of TQ. We found that the esterase
15 activity of HSA is enhanced in ‘N’ isoform in the presence of TQ as compared to ‘B’
16 isoform, while the antioxidant activity is quite significant in ‘B’ isoform. The overall
17 antioxidant activity of HSA is enhanced in the presence of TQ. Thus, the phenolic
18 compound TQ which is a component of *Nigella sativa* has a great potential to bind
19 HSA and induces its free radical scavenging activity. This study provides insight into
20 HSA-TQ interaction, which is of great importance in understanding the chemico-
21 biological interactions for drug-designing, pharmacy and biochemistry.

22

23

1 Acknowledgement

2 MI is highly thankful to Indian Council of Medical Research (ICMR), New Delhi, for
3 financial support in the form of senior research fellowship (BIC/11(12)/2013) and
4 Grant (No. BMS-58/14/2006). GR is highly thankful to Council of Scientific and
5 Industrial Research, New Delhi, India for financial support in the form of Research
6 Associateship. The authors would like thank to Interdisciplinary Biotechnology Unit,
7 Aligarh Muslim University for providing instrumental facilities.

8

9 Reference

- 10 1. M. M. Abukhader, *Pharmacogn Rev*, 2013, **7**, 117-120.
- 11 2. M. El Gazzar, R. El Mezayen, J. C. Marecki, M. R. Nicolls, A. Canastar and S. C.
12 Dreskin, *Int Immunopharmacol*, 2006, **6**, 1135-1142.
- 13 3. D. Dey, R. Ray and B. Hazra, *Phytother Res*, 2013.
- 14 4. Y. S. Chen, H. M. Yu, J. J. Shie, T. J. Cheng, C. Y. Wu, J. M. Fang and C. H. Wong,
15 *Bioorg Med Chem*, 2014, **22**, 1766-1772.
- 16 5. R. Sedaghat, M. Roghani and M. Khalili, *Iran J Pharm Res*, 2014, **13**, 227-234.
- 17 6. K. S. Siveen, N. Mustafa, F. Li, R. Kannaiyan, K. S. Ahn, A. P. Kumar, W. J. Chng
18 and G. Sethi, *Oncotarget*, 2014, **5**, 634-648.
- 19 7. K. Wallevik, *J Biol Chem*, 1973, **248**, 2650-2655.
- 20 8. J. R. Lakowicz, 1983, **Plenum Press, New York, London**, p.237.
- 21 9. N. El-Najjar, R. A. Ketola, T. Nissila, T. Mauriala, M. Antopolsky, J. Janis, H. Gali-
22 Muhtasib, A. Urtti and H. Vuorela, *J Chem Biol*, 2010, **4**, 97-107.
- 23 10. G. Sudlow, D. J. Birkett and D. N. Wade, *Mol Pharmacol*, 1976, **12**, 1052-1061.
- 24 11. X. Z. Feng, Z. Lin, L. J. Yang, C. Wang and C. L. Bai, *Talanta*, 1998, **47**, 1223-
25 1229.
- 26 12. W. C. Johnson, Jr., *Proteins*, 1990, **7**, 205-214.
- 27 13. G. Lupidi, A. Scire, E. Camaioni, K. H. Khalife, G. De Sanctis, F. Tanfani and E.
28 Damiani, *Phytomedicine*, 2010, **17**, 714-720.
- 29 14. J. M. Salmani, S. Asghar, H. Lv and J. Zhou, *Molecules*, 2014, **19**, 5925-5939.
- 30 15. S. S. Ulasli, S. Celik, E. Gunay, M. Ozdemir, O. Hazman, A. Ozyurek, T. Koyuncu
31 and M. Unlu, *Asian Pac J Cancer Prev*, 2013, **14**, 6159-6164.
- 32 16. H. Gali-Muhtasib, M. Diab-Assaf, C. Boltze, J. Al-Hmaira, R. Hartig, A. Roessner
33 and R. Schneider-Stock, *Int J Oncol*, 2004, **25**, 857-866.
- 34 17. S. E. Hassanien, A. M. Ramadan, A. Z. Azeiz, R. A. Mohammed, S. M. Hassan, A.
35 M. Shokry, A. Atef, K. B. Kamal, S. Rabah, J. S. Sabir, O. A. Abuzinadah, F. M. El-
36 Domyati, G. B. Martin and A. Bahieldin, *C R Biol*, 2013, **336**, 546-556.

- 1 18. S. P. Vaillancourt F, Shi Q, Fahmi H, Fernandes JC, Benderdour M., *J. Cell*
2 *Biochem.* , 2010.
- 3 19. R. L. Gurung, S. N. Lim, A. K. Khaw, J. F. Soon, K. Shenoy, S. Mohamed Ali, M.
4 Jayapal, S. Sethu, R. Baskar and M. P. Hande, *PLoS One*, 2010, **5**, e12124.
- 5 20. K. M. Sutton, A. L. Greenshields and D. W. Hoskin, *Nutr Cancer*, 2014, **66**, 408-
6 418.
- 7 21. A. A. Fouad and I. Jresat, *Andrologia*, 2014.
- 8 22. A. Ragheb, A. Attia, W. S. Eldin, F. Elbarbry, S. Gazarin and A. Shoker, *Saudi J*
9 *Kidney Dis Transpl*, 2009, **20**, 741-752.
- 10 23. T. Peters, Jr., *Adv Protein Chem*, 1985, **37**, 161-245.
- 11 24. M. Ishtikhar, G. Rabbani and R. H. Khan, *Colloids Surf. B: Biointerfaces*, 2014.
- 12 25. A. Varshney, M. Rehan, N. Subbarao, G. Rabbani and R. H. Khan, *PLoS One*, 2011,
13 **6**, e17230.
- 14 26. J. Hodgson, *Nat Biotechnol*, 2001, **19**, 897-898.
- 15 27. E. Ahmad, G. Rabbani, N. Zaidi, S. Singh, M. Rehan, M. M. Khan, S. K. Rahman,
16 Z. Quadri, M. Shadab, M. T. Ashraf, N. Subbarao, R. Bhat and R. H. Khan, *PLoS*
17 *One*, 2011, **6**, e26186.
- 18 28. U. Anand, C. Jash and S. Mukherjee, *J Phys Chem B*, 2010, **114**, 15839-15845.
- 19 29. M. Ishtikhar, S. Khan, G. Badr, A. Osama Mohamed and R. Hasan Khan, *Mol*
20 *Biosyst*, 2014, **10**, 2954-2964.
- 21 30. J. E. Ladbury and M. A. Williams, *Curr Opin Struct Biol*, 2004, **14**, 562-569.
- 22 31. Y. H. Chen, J. T. Yang and H. M. Martinez, *Biochemistry*, 1972, **11**, 4120-4131.
- 23 32. G. Rabbani, E. Ahmad, N. Zaidi, S. Fatima and R. H. Khan, *Cell Biochem Biophys*,
24 2012, **62**, 487-499.
- 25 33. F. r. T, *Ann Phys*, 1948, **2**, 55-75.
- 26 34. P. J. Il'ichev YV, Simon JD, *J Phys Chem B*, 2002, **116**, 452-459.
- 27 35. G. M. Zhao Hongwei, Zhang Zhaoxia, Wang Wenfeng, Wu Guozhong,
28 *Spectrochimica Acta: A*, 2005, **65**, 811-817.
- 29 36. R. K. Belew, & Olson, A. J., *Journal of Computational Chemistry*, 1998, **19**, 1639-
30 1645.
- 31 37. M. F. Sanner, *J Mol Graph Model*, 1999, **17**, 57-61.
- 32 38. E. F. Pettersen, T. D. Goddard, C. C. Huang, G. S. Couch, D. M. Greenblatt, E. C.
33 Meng and T. E. Ferrin, *J Comput Chem*, 2004, **25**, 1605-1612.
- 34 39. M. T. Rehman, H. Shamsi and A. U. Khan, *Mol Pharm*, 2014, **11**, 1785-1797.
- 35 40. R. Re, N. Pellegrini, A. Proteggente, A. Pannala, M. Yang and C. Rice-Evans, *Free*
36 *Radic Biol Med*, 1999, **26**, 1231-1237.
- 37 41. G. Rabbani, E. Ahmad, N. Zaidi and R. H. Khan, *Cell Biochem Biophys*, 2011, **61**,
38 551-560.
- 39 42. Z. J. Yasseen, J. H. Hammad and A. L. HA, *Spectrochim Acta A Mol Biomol*
40 *Spectrosc*, 2014, **124**, 677-681.
- 41 43. P. D. Ross and S. Subramanian, *Biochemistry*, 1981, **20**, 3096-3102.
- 42 44. A. A. Thoppil, R. Sharma and N. Kishore, *Biopolymers*, 2008, **89**, 831-840.
- 43 45. Z. Chi and R. Liu, *Biomacromolecules*, 2011, **12**, 203-209.
- 44 46. G. Zolotnitsky, U. Cogan, N. Adir, V. Solomon, G. Shoham and Y. Shoham, *Proc*
45 *Natl Acad Sci U S A*, 2004, **101**, 11275-11280.

- 1 47. K. Takeda, A. Wada, K. Yamamoto, Y. Moriyama and K. Aoki, *J Protein Chem*,
2 1989, **8**, 653-659.
- 3 48. C. Giancola, C. De Sena, D. Fessas, G. Graziano and G. Barone, *Int J Biol*
4 *Macromol*, 1997, **20**, 193-204.
- 5 49. S. S. Sinha, R. K. Mitra and S. K. Pal, *J Phys Chem B*, 2008, **112**, 4884-4891.
- 6 50. A. I. Luik, N. Naboka Yu, S. E. Mogilevich, T. O. Hushcha and N. I. Mischenko,
7 *Spectrochim Acta A Mol Biomol Spectrosc*, 1998, **54A**, 1503-1507.
- 8 51. L. A. Hushcha TO, Naboka YN., *Talanta*, 2000, **2**, 29-34.
- 9 52. Y. J. Hu, Y. Liu, T. Q. Sun, A. M. Bai, J. Q. Lu and Z. B. Pi, *Int J Biol Macromol*,
10 2006, **39**, 280-285.
- 11 53. J. N. Miller, *Proc Anal Div Chem Soc*, , 1979, **16**, 203-208.
- 12 54. S. Bi, Song, D., Kan, Y., Xu, D., Tian, Y., Zhou, X., Zhang, H., *Acta A Mol. Biomol.*
13 *Spectrosc*, 2005, **62**, 203-212.
- 14 55. Y. Li, X. Yao, J. Jin, X. Chen and Z. Hu, *Biochim Biophys Acta*, 2007, **1774**, 51-58.
- 15 56. S. H. Volland C, Dammeyer J, Benet LZ, *Drug Metab Dispos*, 1991, **19**, 1080-1086.
- 16 57. P. C. Smith, W. Q. Song and R. J. Rodriguez, *Drug Metab Dispos*, 1992, **20**, 962-
17 965.
- 18 58. B. C. Sallustio, B. A. Fairchild and P. R. Pannall, *Drug Metab Dispos*, 1997, **25**, 55-
19 60.
- 20 59. L. F. Dubois-Presle N1, Maurice MH, Fournel-Gigleux S, Magdalou J, Abiteboul M,
21 Siest G, Netter P., *Mol Pharmacol*, 1995, **47**, 5647-5653.
- 22 60. K. Staniek, T. Rosenau, W. Gregor, H. Nohl and L. Gille, *Biochem Pharmacol*,
23 2005, **70**, 1361-1370.
- 24 61. H. Hosseinzadeh, S. Parvardeh, M. N. Asl, H. R. Sadeghnia and T. Ziaee,
25 *Phytomedicine*, 2007, **14**, 621-627.
- 26 62. S. Padhye, S. Banerjee, A. Ahmad, R. Mohammad and F. H. Sarkar, *Cancer Ther*,
27 2008, **6**, 495-510.
- 28 63. Z. Solati, B. S. Baharin and H. Bagheri, *J Am Oil Chem Soc*, 2014, **91**, 295-300.
- 29 64. H. Gali-Muhtasib, A. Roessner and R. Schneider-Stock, *Int J Biochem Cell Biol*,
30 2006, **38**, 1249-1253.
- 31 65. S. Chandra, S. N. Murthy, D. Mondal and K. C. Agrawal, *Can J Physiol Pharmacol*,
32 2009, **87**, 300-309.
- 33 66. M. N. Nagi and M. A. Mansour, *Pharmacol Res*, 2000, **41**, 283-289.
- 34 67. M. N. Nagi, K. Alam, O. A. Badary, O. A. al-Shabanah, H. A. al-Sawaf and A. M.
35 al-Bekairi, *Biochem Mol Biol Int*, 1999, **47**, 153-159.
- 36 68. O. A. Badary, R. A. Taha, A. M. Gamal el-Din and M. H. Abdel-Wahab, *Drug*
37 *Chem Toxicol*, 2003, **26**, 87-98.
- 38 69. H. Lee, M. K. Cha and I. H. Kim, *Arch Biochem Biophys*, 2000, **380**, 309-318.
- 39 70. K. Oettl and R. E. Stauber, *Br J Pharmacol*, 2007, **151**, 580-590.
- 40 71. M. Taverna, A. L. Marie, J. P. Mira and B. Guidet, *Ann Intensive Care*, 2013, **3**, 4.
- 41 72. B. Özcelik, Lee, J.H., Min, D.B., *Journal of Food Sciences*, 2003, **68**, 1361-1370.
- 42 73. I. Gulcin, *Life Sci*, 2006, **78**, 803-811.
- 43

44

Table 1: Binding and thermodynamic parameters of HSA and TQ at different temperatures obtained from fluorescence quenching experiments and ITC.

	pH/isoform	Temp. (°C)	K_{sv} ×10 ⁴ (M ⁻¹)	k_q ×10 ¹² (M ⁻¹ s ⁻¹)	n	K_b ×10 ⁴ (M ⁻¹)	ΔG° (kcal mol ⁻¹)	ΔH° (kcal mol ⁻¹)	TΔS° (kcal mol ⁻¹ K ⁻¹)	Dominating forces Involve (inferred)		
5	pH 7.4/N	15	2.45	4.23	1.01	3.08	-5.90		0.80	H-bonding, Hydrophobic interactions		
6		25	2.11	3.65	1.00	2.30	-5.93	-5.10	0.83			
7		37	1.15	1.98	1.02	1.63	-5.97		0.87			
8		45	0.85	1.47	0.99	0.82	-5.99		0.89			
9	NaCl (0.15 M)	37	0.98	1.69	1.01	1.24	-5.80					
10	pH 9.0/B	15	0.55	0.09	0.98	0.44	-4.79		1.08			
11		25	0.35	0.06	0.99	0.34	-4.82	-3.71	1.11			
12		37	0.27	0.04	1.01	0.28	-4.87		1.16			
13		45	0.08	0.01	1.08	0.27	-4.90		1.19			
14	Values obtain by ITC	pH 7.4/N	37			1.01± 0.14	-127.55	-63.50 ± 2.48	-63.55*		H-bonding, Conformational changes	
15						pH 9.0/B	37	0.58± 0.07	-75.01			-37.05 ± 1.58
16	K _{sv} = Stern-Volmer constant; k _q = bimolecular rate constant;											
17	n = stoichiometry of binding;											
18	K _b = binding constant;											
19	ΔG° = change in free energy;											
20	ΔH° = change in enthalpy;											
21	TΔS° = change in entropy;											
22	*kcal/mol/deg.											

1
2
3
4
5
6
7
8
9
10
11
12
13
14
15
16
17
18
19
20
21
22
23
24
25
26

Table 2: Secondary structural analysis to determine the percent structural change in the isoforms of HSA and HSA-TQ complexed.

pH/isoform	HSA(μ M)	TQ (μ M)	% increment in α -helix	T _m ($^{\circ}$ C)
pH 7.4/N	02	00	0	68.18
	02	10	4	72.35
	02	50	9	72.66
pH 9.0/B	02	00	0	72.81
	02	10	9	74.24
	02	50	18	75.02

1

2

3

4

5

6

7

Table 3: Characteristics of hydrodynamic radii (R_h) and polydispersity (P_d) distribution of

8

HSA solution in absence and presence of TQ at pH 7.4 and pH 9.0.

9

pH/isoform	HSA:TQ	R_h (nm)	Change in R_h (%)	P_d (%)
pH 7.4/N	1:00	4.0	100	16.0
	1:05	4.2	105	16.2
	1:25	4.4	110	19.6
pH 9.0/B	1:00	3.6	100	17.4
	1:05	3.8	106	13.9
	1:25	4.0	111	17.6

17

18

19

20

21

22

23

24

25

26

27

28

29

30

31

1
2
3
4
5
6
7
8
9
10
11
12
13
14
15
16
17
18
19
20
21
22
23
24
25
26
27
28
29
30
31

Table 4: FRET data obtained from spectral overlap of HSA emission and TQ absorption at 37 °C.

Variables	pH 7.4	pH 9.0
F	142.862	200.044
F ₀	205.504	232.628
E _{FRET}	0.3048	0.1400
J (cm ³ M ⁻¹)	3.24×10 ⁻¹⁴	2.702×10 ⁻¹⁵
R ₀ (nm)	2.981	1.970
r (nm)	3.42	2.66

1
2
3
4
5
6
7
8
9
10
11
12
13
14
15
16
17
18**Table 5:** Kinetic parameters for the hydrolysis of *p*-nitrophenyl acetate by HSA.

pH/isoform	System	RA (%)	V_{max} (M/min)	K_m (M)	k_{cat} (min⁻¹)	k_{cat}/K_m (M⁻¹ min⁻¹)
pH 7.4/N	HSA	100	4.27×10^{-8}	6.66×10^{-6}	0.854×10^{-2}	1.28×10^3
	HSA+TQ	127	5.42×10^{-8}	9.37×10^{-6}	1.048×10^{-2}	1.11×10^3
pH 9.0/B	HSA	100	6.70×10^{-7}	8.55×10^{-5}	13.41×10^{-2}	1.56×10^3
	HSA + TQ	113	5.12×10^{-7}	4.09×10^{-5}	10.24×10^{-2}	2.50×10^3

1 **Figure captions**

2 **Figure 1:** UV-visible absorption spectra of HSA (6 μM) in absence and presence (00 μM -30 μM)
3 of TQ at (A) pH 7.4; (B) pH 9.0, respectively.

4 **Figure 2:** (A-I and B-I) the Stern-Volmer plots for the HSA-TQ interaction of N isoform pH 7.4
5 and B isoform pH 9.0 at 15, 25, 37, 45 $^{\circ}\text{C}$ and in presence of 0.15 N NaCl at 37 $^{\circ}\text{C}$. (A-II and B-II)
6 Plot of $\log [(F_0/F)-1]$ vs $\log[Q]$ for the determination of binding constants and binding
7 stoichiometry for HSA-TQ interaction at pH 7.4 at 15, 25, 37, 45 $^{\circ}\text{C}$ and in presence of 0.15 N
8 NaCl at 37 $^{\circ}\text{C}$ at pH 7.4.

9 **Figure 3:** Isothermal titration calorimetric profile of HSA in presence of TQ at pH 7.4 (A) and pH
10 9.0 (B) at 37 $^{\circ}\text{C}$. Titration of TQ with HSA shows calorimetric response as successive titrations of
11 TQ to the sample cell.

12 **Figure 4:** Far-UV CD spectra of HSA (2 μM) in absence and presence of TQ at pH 7.4 (4-IA) and
13 pH 9.0(4-IB). Far-UV CD thermal unfolding spectra of HSA (2 μM) in the absence and presence
14 of TQ in molar ratio of 1:05 and 1:25 at pH 7.4 (4-IIA) and pH 9.0 (4-IIB), respectively.

15 **Figure 5:** Dynamic light scattering of HSA-TQ complex. (5-I) Determination of hydrodynamic
16 radii (R_h) of HSA in the absence and presence of TQ (HSA:TQ molar ratio 1:0, 1:5 and 1:25); A-I,
17 A-II, A-III and B-I, B-II, B-III for pH 7.4 and pH 9.0 respectively. (5-II) TQ concentration
18 dependent changes in hydrodynamic radii of HSA at both pH, shows that hydrodynamic radii
19 increases on increasing the concentration of TQ at both pH.

20 **Figure 6:** Tryptophan fluorescence resonance energy transfer. Spectral overlap of the fluorescence
21 emission of HSA ($\lambda_{\text{ex}} = 295 \text{ nm}$) and absorption spectra of TQ [HSA = TQ = 2 μM] at (A) pH 7.4;
22 (B) pH 9.0, respectively.

1 **Figure 7:** Three-dimensional fluorescence spectra of HSA (2 μ M) in absence (A and B) and
2 presence (A-I and B-I) of TQ at pH 7.4 and pH 9.0, respectively. [HSA: TQ =1:1].

3 **Figure 8:** Molecular docking results (A) TQ represented as ball and stick model and HSA in
4 ribbon, (B) Hydrogen bonding between Tyr150 and Trp214 with TQ in the region of binding
5 pocket.

6 **Figure 9:** The effects of concentration of the antioxidant on the inhibition of the ABTS \bullet^+ by trolox
7 and BHA at pH 7.4 and pH 9.0. Absorbance of ABTS radical scavenging activity of different
8 concentrations of HSA, TQ and reference antioxidants as trolox and BHA (ABTS $^+$: 2,20-
9 azinobis(3-ethylbenzthiazoline-6-sulfonic acid) at pH 7.4 (9-IA), pH 9.0 (9-IB). Percent inhibition
10 of standard reference compounds trolox and BHA (9-II) as well as in presence of phenolic
11 compound TQ and protein at particular concentrations at pH 7.4 (9-IIIA) and pH 9.0 (9-IIIB),
12 respectively.

13

14

15

16

17

18

19

20

21

22

23

24

25

26

27

1
2
3
4
5
6
7
8
9
10
11

Illustrations

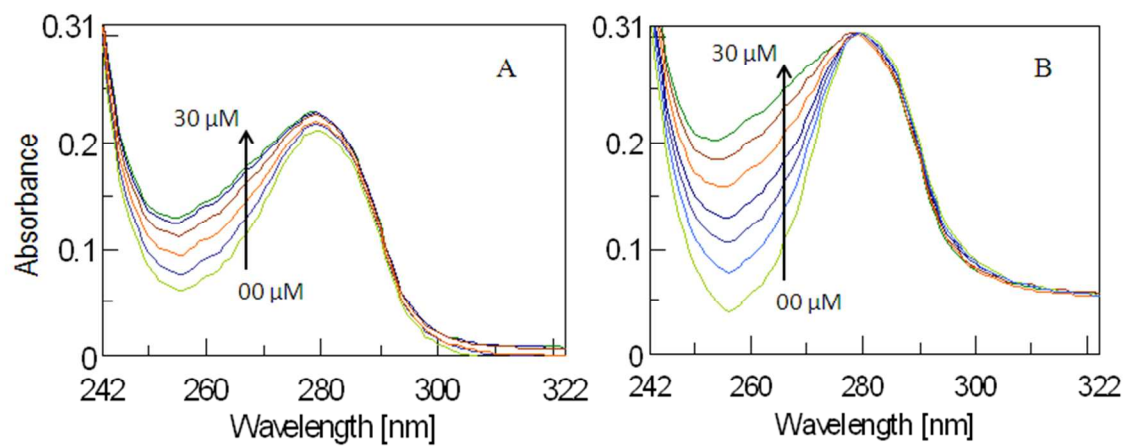


Figure 1

12
13
14
15
16
17
18
19
20
21
22
23
24

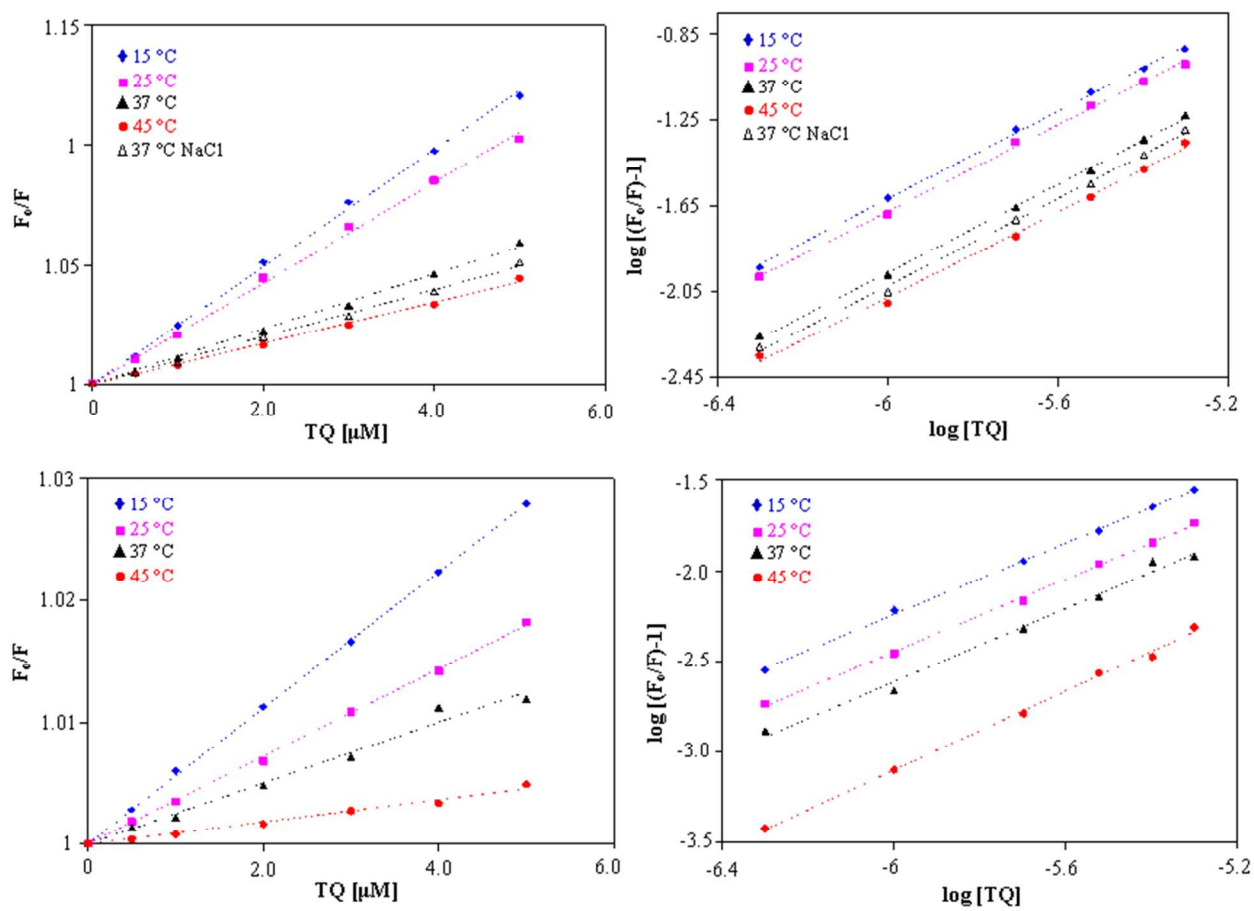
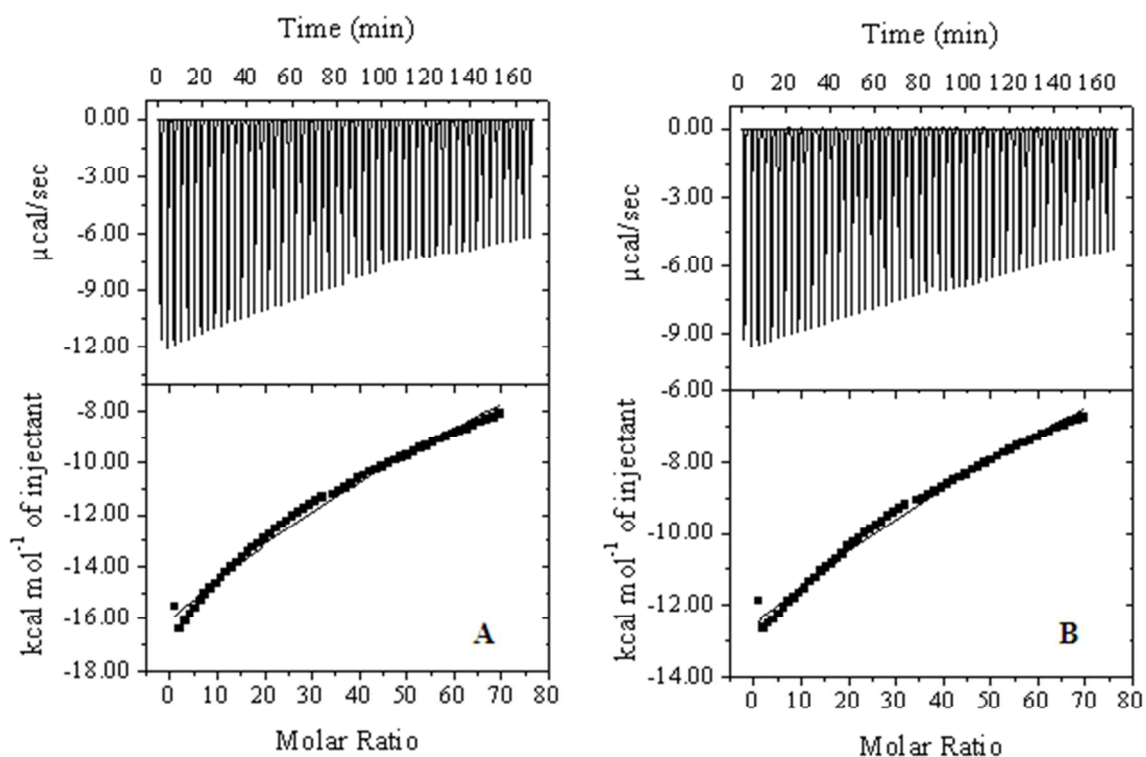
1
2
3
4
5
6
7
89
10
11
12
13
14
15
16

Figure 2

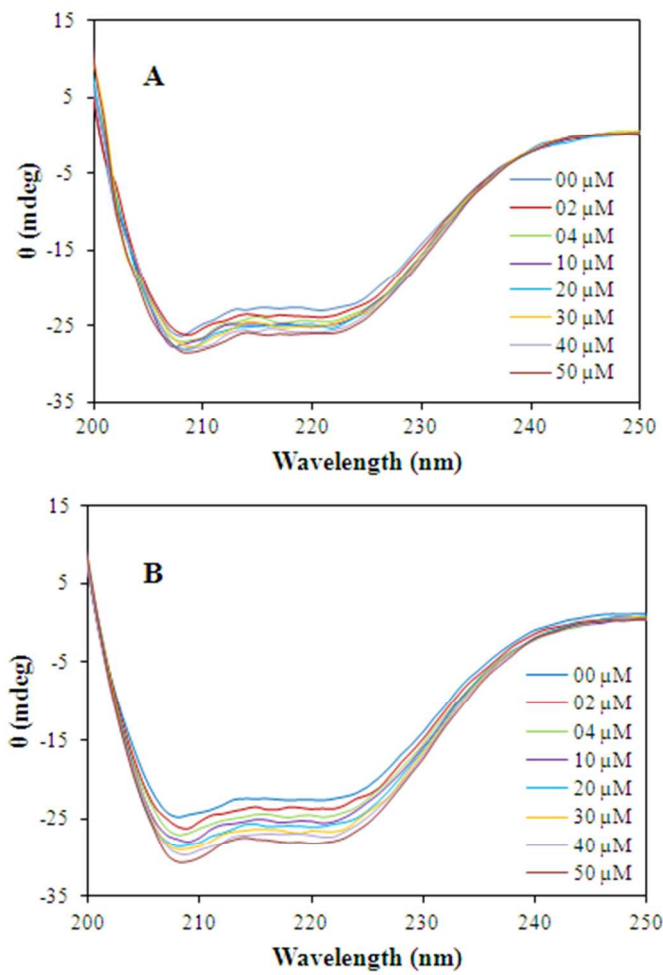
1
2
3
4
5
6
7
8



9
10
11
12
13
14
15
16
17

Figure 3

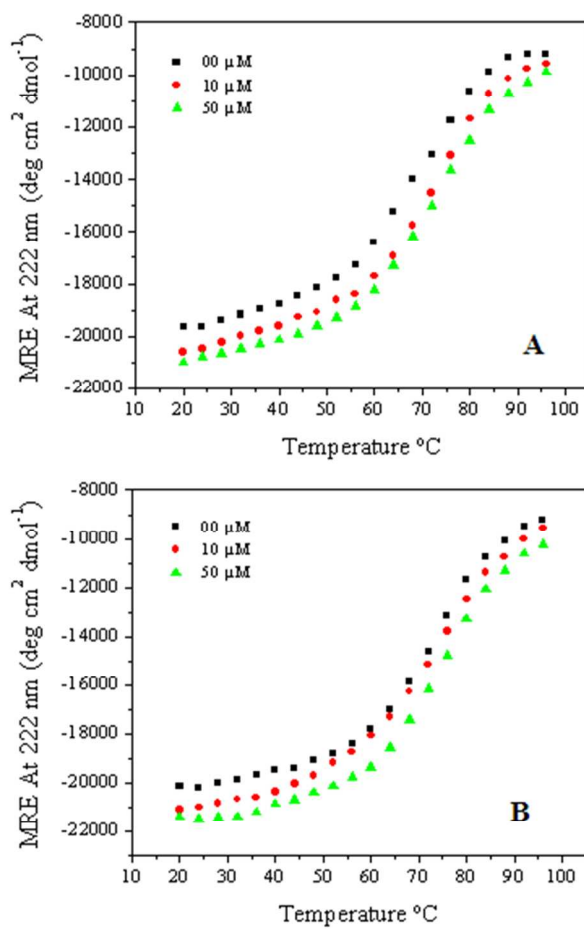
1
2
3
4
5



6
7
8
9
10
11
12
13
14

Figure 4-I

1
2
3
4
5



6
7
8
9
10
11
12
13

Figure 4-II

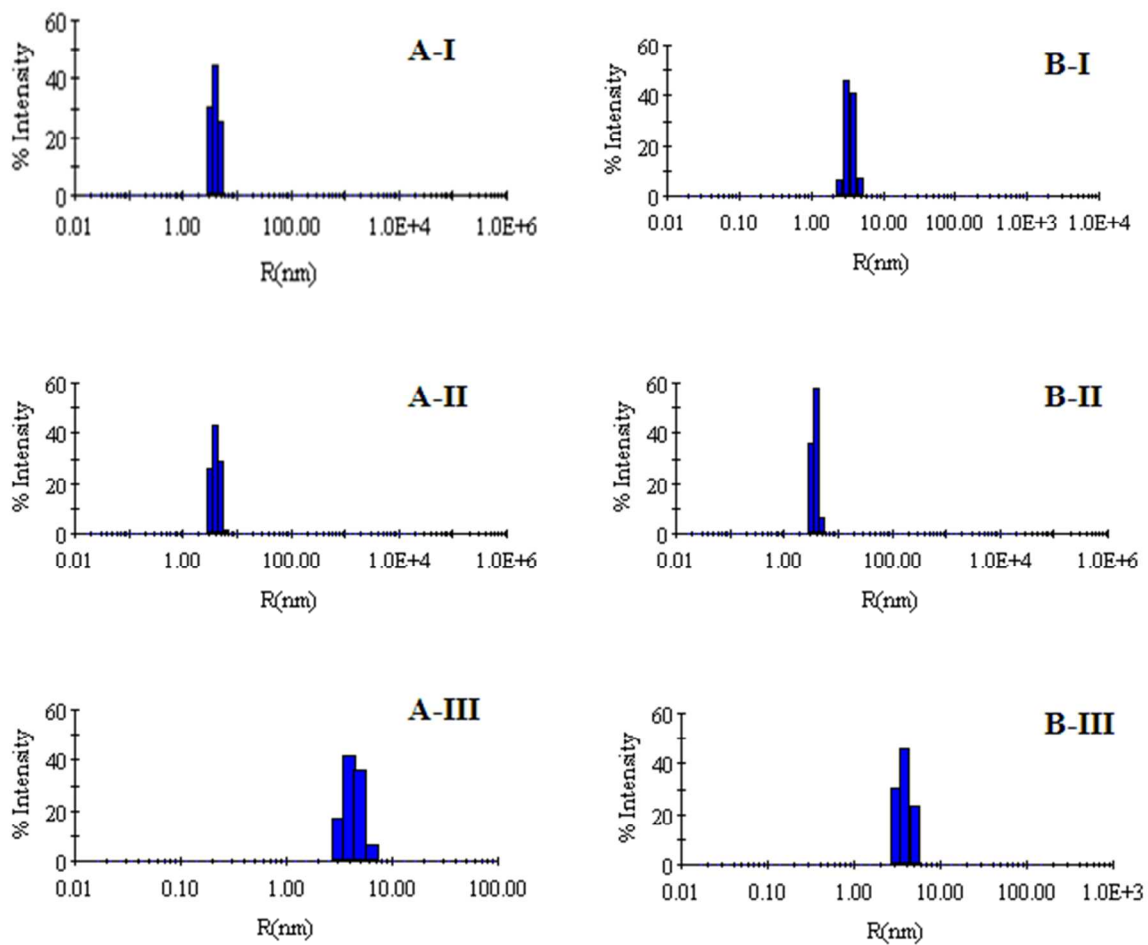
1
2
3
4
5
6
78
9
10
11
12
13

Figure S-1

1
2
3
4
5
6
7

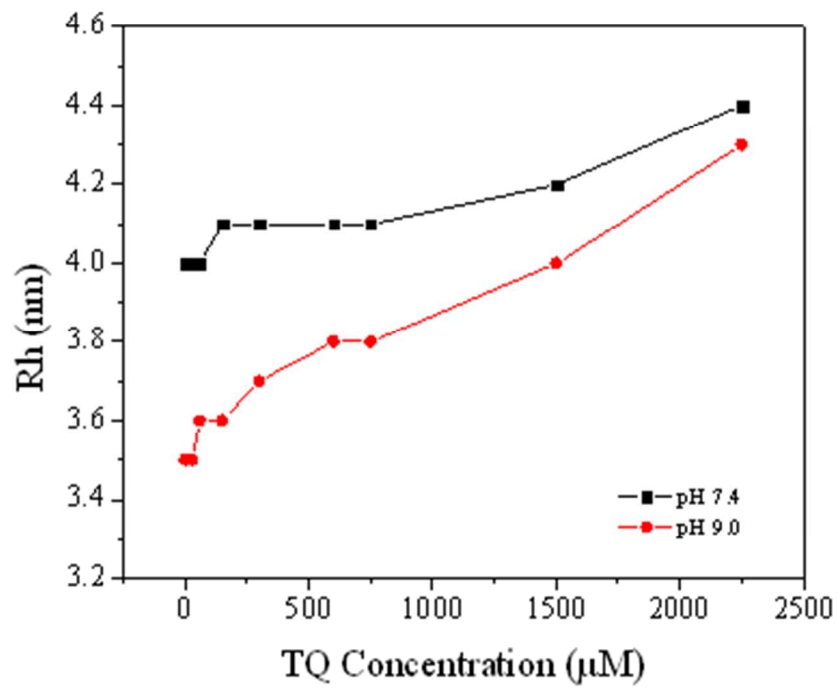
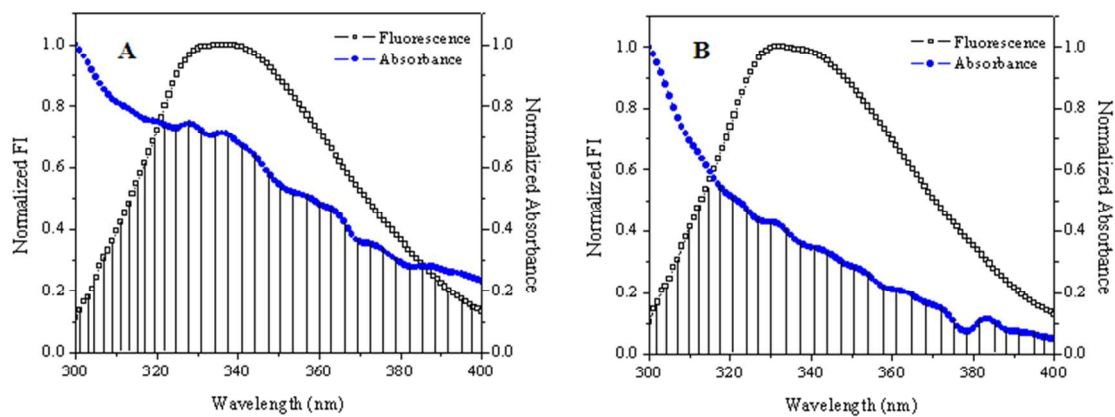


Figure 5-II

8
9
10
11
12
13
14
15
16
17

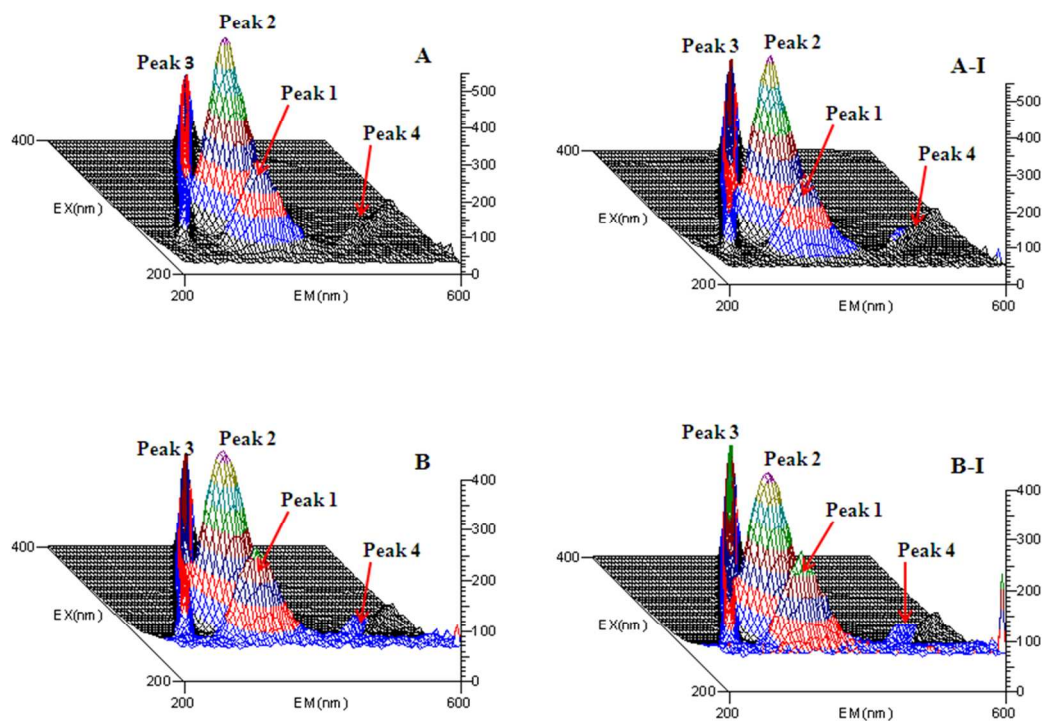
1
2
3
4
5
6
7
8
9



10
11
12
13
14
15
16
17
18
19
20
21
22
23
24

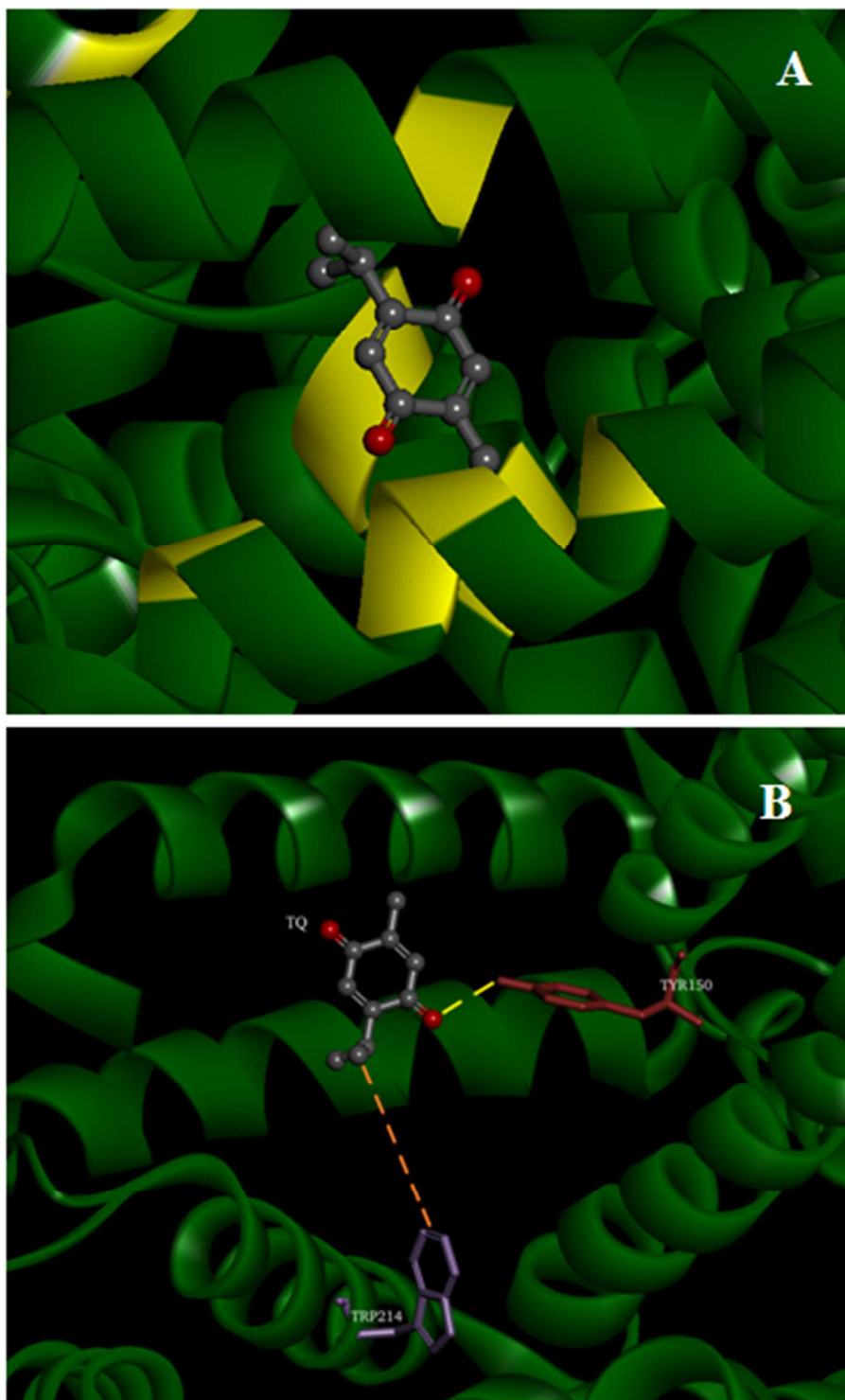
Figure 6

1
2
3
4
5
6



7
8
9
10
11
12

Figure 7



1
2
3
4

Figure 8

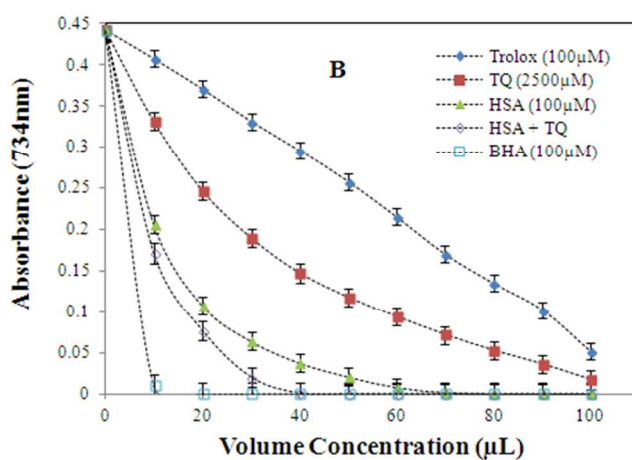
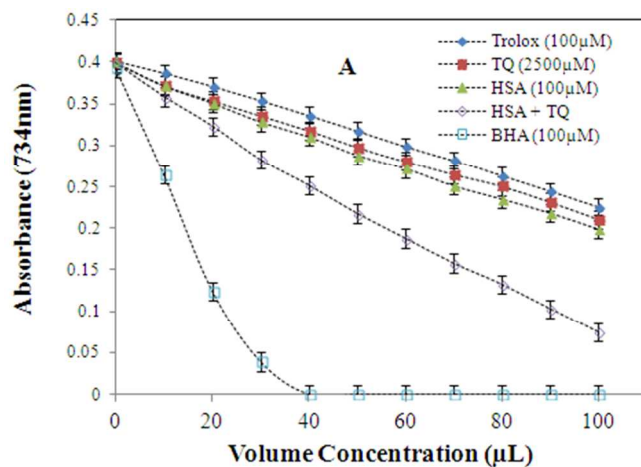


Figure 9-I

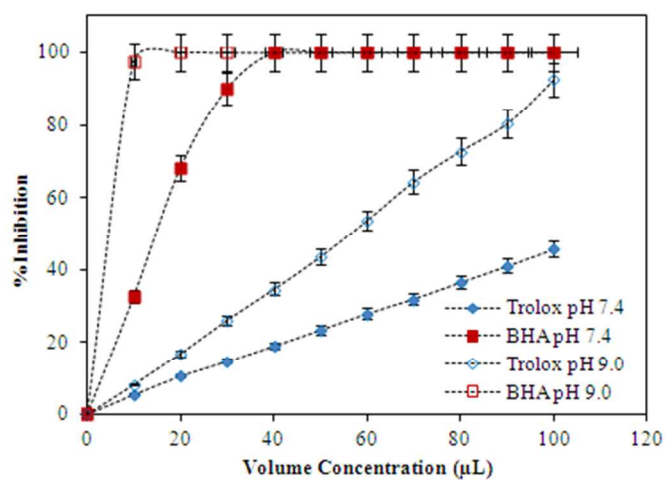
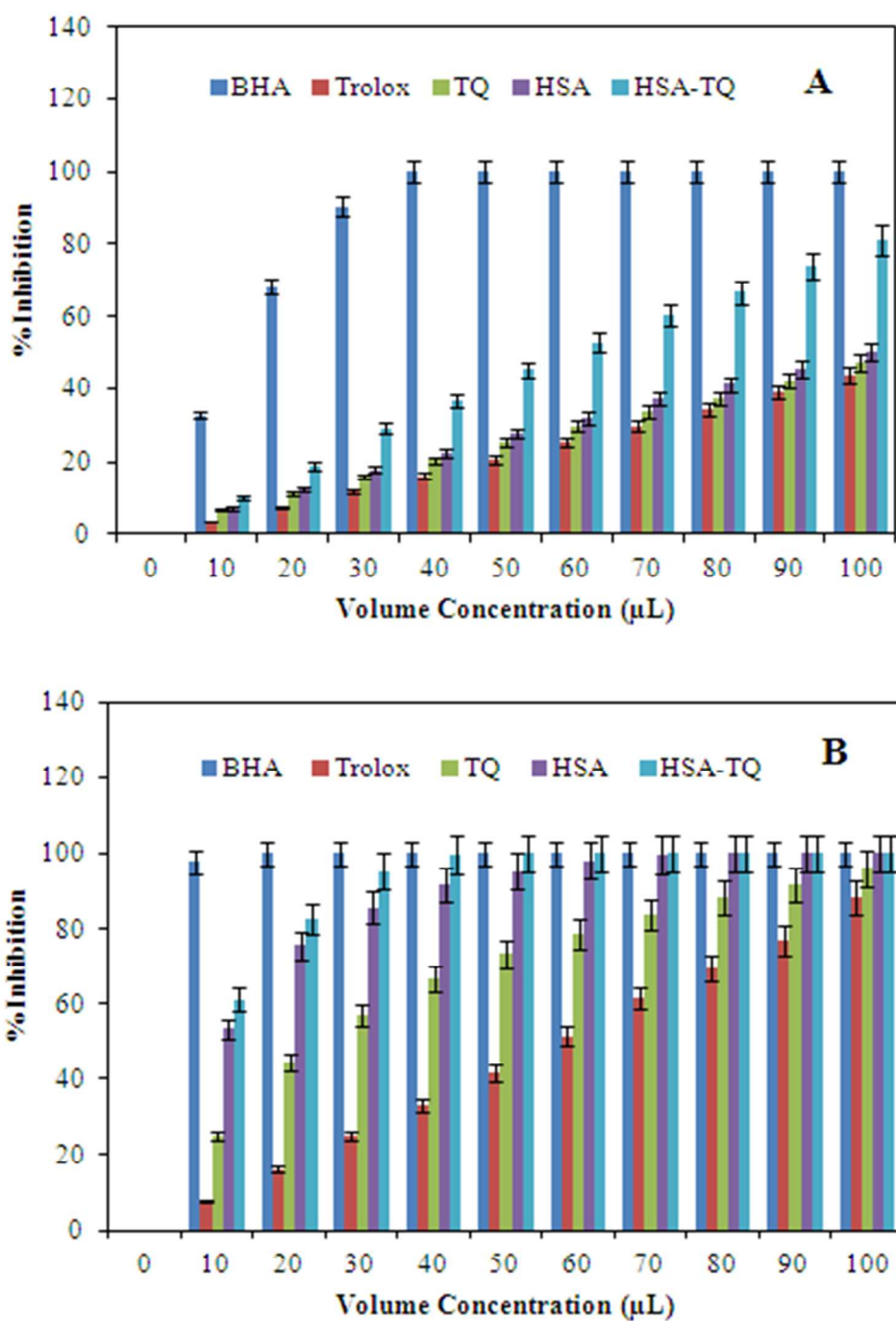


Figure 9-II

1
2
34
5
6

1

2



3

4

5

6

Figure 9-III

1 **Supporting Information description**

2 **Figure S-1:** Fluorescence emission spectra of HSA (2 μM) in presence of TQ (0-25 μM) at (A) pH
3 7.4; (B) pH 9.0.

4 **Figure S-2:** (A) Van't Hoff plot; and (B) Thermodynamic signatures for HSA-TQ interaction in N
5 and B isoforms at 15, 25 and 37 $^{\circ}\text{C}$.

6 **Figure S-3:** The contour of three-dimensional fluorescence spectra of HSA (2 μM) in absence (A
7 and B) and presence (A-I and B-I) of TQ at pH 7.4 and pH 9.0, respectively. [HSA: TQ =1:1].

8 **Figure S-4:** Enzyme kinetics for HSA. The Michaelis-Menton equation based activity against
9 substrate concentrations at a fixed TQ (5 μM) and HSA (5 μM) concentration of HSA and HSA-
10 TQ complex (1:1) at (A) pH 7.4, (B) pH 9.0, respectively.

11 **Table T-1:** Three-dimensional fluorescence spectra characteristics of HSA-TQ interaction at pH
12 7.4 and 9.0

13 **Table T-2:** Comparison between the antioxidant activity of TQ with ABTS^{•+} at specific
14 concentration (aliquot of 100 μL), and at particular time-points.

15

16

17

18

19

20

21

22

23